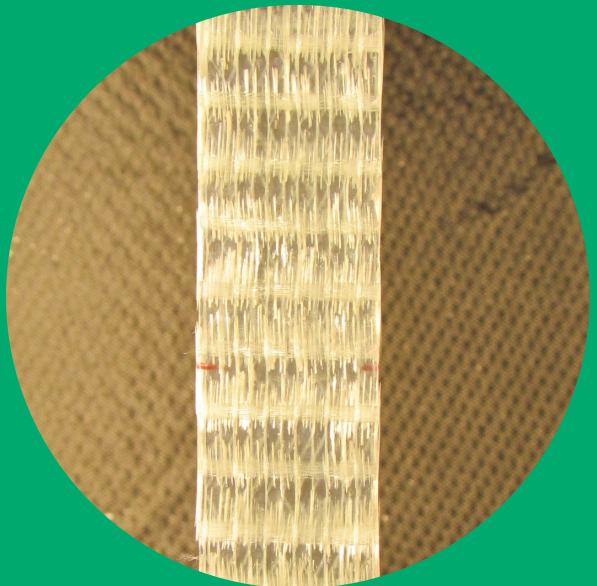# Tensile-tensile fatigue testing and fatigue properties of quasi-unidirectional non-crimp fabric reinforced glass-fibre/epoxy laminates

Samuli Korkiakoski

Tensile-tensile fatigue testing and fatigue properties of quasi-unidirectional non-crimp fabric reinforced glass-fibre/epoxy laminates

Samuli Korkiakoski

A doctoral dissertation completed for the degree of Doctor of Science (Technology) to be defended, with the permission of the Aalto University School of Engineering, at a public examination held at the lecture hall K216 of the school on 2nd February 2018 at 12.

Aalto University
School of Engineering
Department of Mechanical Engineering

Supervising professor
Prof. Olli Saarela, Aalto University, Finland

Thesis advisor
Prof. Mikko Kanerva, Tampere University of Technology, Finland

Preliminary examiners
Prof. Valter Carvelli, Politecnico di Milano, Italy
Dr. Katleen Vallons, Katholieke Universiteit Leuven, Belgium

Opponent
Prof. Leif Asp, Chalmers University of Technology, Sweden

NORDIC ECOLABEL

441   697
Printed matter

Abstract

This thesis focuses on tensile-tensile fatigue of quasi-unidirectional (quasi-UD) non-crimp fabric (NCF) reinforced glass-fibre/epoxy laminates. These laminates have good fatigue performance since fibre bundles exhibit a very small amount of crimp. They are commonly used in fatigue critical structures, e.g. in spar caps of wind turbine rotor blades.

The thesis is divided into three parts. The first part is devoted to the development of an applicable test specimen configuration for tensile-tensile fatigue testing of the laminates. This is necessary because standard rectangular specimens tend to fail at the tab area, resulting in unrealistic fatigue life predictions. The thesis further focuses on the internal structure characterisation, fatigue damage evolution and fatigue performance of laminates reinforced with NCFs based on different stitch patterns and stitch tensions. The third part concentrates on dry and wet compaction of quasi-UD NCF preforms, with the aim of finding out how the NCF structure and preform thickness possibly affect the final thickness and fibre volume fraction (FVF) of the laminate.

The first part revealed that the developed dog-bone specimen configuration decreased tab failures and yielded significantly higher fatigue lives for UD laminates when compared to the fatigue lives measured with rectangular and slightly different dog-bone specimens. Fatigue tests and mesostructural analyses performed in the second part indicated that damage evolution and the measured fatigue life were significantly dependent on the stitch pattern, while they were not dependent on the stitch tension. The main reasons for the differences were apparently the waviness of axial fibres that were dependent on the stitch pattern but not on the stitch tension. The study also revealed that the mutual location of stitch patterns in neighbouring fabrics affects the fatigue life of the laminates. Finally, the thesis showed that the dry and wet compaction of quasi-UD preform is dependent on the stitch pattern but not on the stitch tension. In addition, the fabric shift perpendicular to the axial fibre bundles had a small effect on the thickness of the preform.

The results of the first part suggest that the developed specimen configuration is applicable for fatigue tests and provides more reliable fatigue lives for quasi-UD laminates when compared to the reference specimens. However, even with this configuration, part of the specimens failed outside the gauge section, meaning that there is a need for further development of the specimen. The results of the second part revealed that stitch patterns that keep fibre bundles well-aligned provide the best fatigue lives for the laminates. The results also revealed that the mutual location of neighbouring fabrics might affect the fatigue life of the laminates. Thus, the locations should be the same, e.g. when the objective is to compare the fatigue lives of laminates with different stitch patterns and tensions. The results in the third part indicated that FVFs of thin test laminates for fatigue tests correspond well to the FVFs of thicker laminates used in the compaction tests.

Tekijä
Samuli Korkiakoski

Väitöskirjan nimi
Näennäisesti yhdensuuntaisten suorakuitulujitettujen lasikuitu-epoksilaminaattien vetoväsytystestaus ja väsymisominaisuudet

Julkaisija Insinööritieteiden korkeakoulu

Yksikkö Konetekniikan laitos

Sarja Aalto University publication series DOCTORAL DISSERTATIONS 236/2017

Tutkimusala Lentotekniikka

Tiivistelmä

Väitöskirjatutkimus keskittyy näennäisesti yhdensuuntaisista suorakuitulujitteista valmistettujen lasikuitu-epoksilaminaattien vetoväsytystestaukseen. Tällaisilla laminaateilla on hyvät väsymisominaisuudet, koska kuitukimppujen mutkaisuus on hyvin pientä. Niitä käytetään esimerkiksi tuulimyllyjen lapojen kuormaa kantavissa salkorakenteissa.

Väitöskirja jakautuu kolmeen osaan. Ensimmäisessä osassa keskitytään vetoväsytystestaukseen soveltuvan, mitta-alueeltaan kavennetun koesauvakonfiguraation kehittämiseen, sillä standardoidut suorakaiteen muotoiset koesauvat hajoavat usein päätyvahvikkeista tuottaen epärealistisia väsymiselinikiä. Toisessa osassa keskitytään suorakuitulujitteilla lujitettujen laminaattien sisäisen rakenteen tutkimiseen sekä laminaattien väsymisvaurioitumisen ja väsymiskestävyyden tutkimiseen. Kolmannessa osassa tutkitaan suorakuitulujitteista muodostettujen lujiteaihioiden kuiva- ja märkäpakkautuvuutta.

Väitöskirjan ensimmäinen osa osoitti, että kehitetty koesauva vähentää yhdensuuntaisen laminaatin päätyvahvikevaurioita ja sietää merkittävästi enemmän kuormitussyklejä kuin standardin mukainen suorakaiteen muotoinen koesauva ja kehitetystä koesauvasta hieman poikkeava kavennettu koesauva. Toisen osan koetulosten mukaan suorakuitulujitteen tikkausparametreista tikin muoto vaikuttaa, mutta tikin kireys ei vaikuta laminaatissa väsytysvaurioiden kehittymiseen ja mitattuun elinikään. Merkittävin syy eroavaisuuksiin on oletettavasti kuitujen mutkittelu, joka riippuu tikin muodosta, mutta ei sen kireydestä. Koetulokset osoittivat myös, että tikkauksen sijainti vierekkäisen lujitteen tikkaukseen nähden vaikuttaa laminaatin elinikään. Kolmannen osan tulokset osoittivat, että tikin muoto vaikuttaa, mutta tikin kireys ei vaikuta lujiteaihion paksuuteen pakkautuvuuskokeissa. Tulokset osoittivat myös, että pitkittäisten kuitukimppujen keskinäinen asema vaikuttaa hieman lujiteaihion paksuuteen.

Väitöskirjan ensimmäisen osan tulokset osoittavat, että kehitetty kavennettu koesauvakonfiguraatio on soveltuva väsytystestaukseen, sillä se tuottaa realistisempia elinikiä verrattuna referenssikoesauvoihin. Osa koesauvoista kuitenkin rikkoontui mitta-alueen ulkopuolelta, joten koesauvan jatkokehitys on yhä tarpeen. Toisen osion tulokset paljastivat, että laminaattien paras väsymiskestävyys saavutetaan tikkimuodolla, joka pitää kuitukimput mahdollisimman suorassa. Tulokset myös osoittivat, että kuitukimppujen keskinäinen sijainti saattaa vaikuttaa laminaatin elinikään. Siksi lujitteiden keskinäisen sijainnin tulisi olla sama, kun vertaillaan eri tikkausparametreilla valmistettujen suorakuitulujitteisten laminaattien elinikiä. Kolmannen osan tulokset osoittivat, että ohuiden väsytyskoelaminaattien kuitupitoisuudet vastaavat hyvin pakkautuvuuskokeissa tutkittujen paksumpien laminaattien kuitupitoisuuksia.

Preface

Many different people have made this thesis possible. I sincerely thank my supervising Professor Olli Saarela for offering me the opportunity to do the research work and for valuable support, encouragement, and guidance throughout the project. I am also grateful to my advisor, Professor Mikko Kanerva, for being a motivational person and for giving fresh ideas especially at the end part of the work. I wish to thank all colleagues of Laboratory of Lightweight Structures for your great help and being involved in many fruitful discussions with this research topic. I also wish to thank personnel from Tampere University of Technology who performed some experiments for this work. Especially, I want to thank Professor Essi Sarlin for her great comments and ideas during the project. I would also like to acknowledge Dr. Maija Hoikkanen, Jukka Koulu and Rainer Bergström from Ahlstrom-Munksjö Oyj for giving valuable practical information about the research topic and supplying raw materials for the study.

I would also like to acknowledge the pre-examiners of this thesis, Professor Valter Carvelli and Dr. Katleen Vallons, and the opponent Professor Leif Asp for their efforts.

I wish to thank my parents, siblings and friends for their support. Last but not least, I would like to express my deepest gratitude to my wife Maria with her priceless support and patience during the whole work. Without you, the work would never have been completed. In addition, special thanks go to my children Elia, Edit and Signe. You delighted me every day and gave me new power and joy to do this work.

Espoo, November 2017
Samuli Korkiakoski

Contents

List of Abbreviations and Symbols

A	Amplitude
A_w	Areal weight of fabric
C	Intercept parameter
h	Thickness of preform
m	Slope of *S-N* curve
N	Number of cycles
n	Number of fabrics
S	Maximum applied stress
V_f	Fibre volume fraction
y'	Maximum slope of tangent
λ	Wavelength
ρ_f	Density of fibre
FE	Finite element
FVF	Fibre volume fraction
GFRP	Glass-fibre-reinforced plastic
NCF	Non-crimp fabric
Quasi-UD	Quasi-unidirectional
SCF	Stress concentration factor
UD	Unidirectional
VI	Vacuum infusion

List of Publications

This doctoral dissertation consists of a summary and the following publications, which are referred to in the text by their numerals.

1. Korkiakoski, Samuli; Brøndsted, Povl; Sarlin, Essi; Saarela, Olli. Influence of specimen type and reinforcement on measured tension–tension fatigue life of unidirectional GFRP laminates. International Journal of Fatigue, Volume 85, pages 114-129, 2016. DOI: 10.1016/j.ijfatigue.2015.12.008.

2. Korkiakoski, Samuli; Sarlin, Essi; Suihkonen, Reija; Saarela, Olli. Internal structure and fatigue performance of quasi-unidirectional Non-Crimp Fabric reinforced laminates. Journal of Composite Materials, Volume 51, pages 3405-3423, 2017. DOI: 10.1177/0021998316683783.

3. Korkiakoski, Samuli; Sarlin, Essi; Suihkonen, Reija; Saarela, Olli. Influence of reinforcement positioning on tension-tension fatigue performance of quasi-unidirectional GFRP laminates made of stitched fabrics. Composites Part B: Engineering, Volume 112, pages 38-48, 2017. DOI: 10.1016/j.compositesb.2016.12.017.

4. Korkiakoski, Samuli; Haavisto, Mikko; Rostami Barouei, Mohammad; Saarela, Olli. Experimental Compaction Characterization of Unidirectional Stitched Non-Crimp Fabrics in the Vacuum Infusion Process. Polymer Composites, Volume 37, Issue 9, pages 2692-2704, 2016. DOI: 10.1002/pc.23464.

Author's Contribution

Publication 1: The author developed a dog-bone specimen and its manufacturing process, prepared all test specimens and carried out quasi-static tensile tests and most of the fatigue tests. He also carried out numerical analyses and statistical analyses and wrote the manuscript. Brøndsted carried out part of the fatigue tests and made valuable comments on the manuscript. Sarlin measured glass transition temperatures and fibre volume fractions of the test laminates. Saarela contributed with valuable comments and suggestions.

Publication 2: The author prepared all test specimens and carried out quasi-static tensile tests and fatigue tests. He also carried out statistical analyses, measured the in-plane waviness of axial fibre bundles and wrote the manuscript. Sarlin and Suihkonen measured glass transition temperatures and fibre volume fractions of the test laminates and took cross-sectional microscope images of the laminates. Saarela contributed with valuable comments and suggestions.

Publication 3: The author prepared all test specimens and carried out quasi-static tensile tests and fatigue tests. He also carried out statistical analyses, measured the in-plane waviness of axial fibre bundles and wrote the manuscript. Sarlin and Suihkonen measured glass transition temperatures and fibre volume fractions of the test laminates and took cross-sectional microscope images of the laminates. Saarela contributed with valuable comments and suggestions.

Publication 4: The author assisted in the development of the compaction test set-up carried out by Rostami Barouei and assisted in compaction tests carried out by Rostami Barouei and Haavisto. The author also carried out part of the compaction tests, analysed the test results and wrote the manuscript. Saarela contributed with valuable comments and suggestions.

Original features

The following features are believed to be original in this thesis:

1) The performed tensile-tensile fatigue tests showed that the developed dog-bone specimen configuration decreased tab failures and yielded significantly higher fatigue lives for unidirectional (UD) glass-fibre reinforced laminates when compared to the fatigue lives measured with rectangular and slightly different dog-bone specimens. The main reasons for the difference in the performances of two dog-bone specimen types were different shear stresses at curved edges of the specimens, different end tab materials and adhesives, and different manufacturing procedures of the specimens. (Publication 1)

2) The tensile-tensile fatigue tests performed for quasi-UD laminates using the developed dog-bone specimen revealed that damage evolution was significantly dependent on the stitch pattern used in the non-crimped fabric. The damage evolution and consequently the fatigue life were not dependent on the stitch tension. Internal structure characterisation of the laminates based on micrographs showed that in-plane and out-of-plane waviness of axial fibres were clearly affected by the stitch pattern but not by the stitch tension. The fibre waviness was lowest in the best-performing laminate with the double-tricot stitch pattern. (Publication 2)

3) The tensile-tensile fatigue tests performed using the developed dog-bone specimen showed that the mutual location of fabrics perpendicular to the axial fibre bundles affected insignificantly the damage development rate and fatigue life of quasi-UD laminates formed from two layers. The laminate with axial fibre bundles on top of each other showed a similar damage development rate and fatigue life when compared to the laminate with the fibre bundles overlapping. The mutual location of the fabrics parallel to the axial bundles had a significant effect on the damage development rate and fatigue performance. The laminate with a reversed stitch phase between the fabrics showed a considerably lower damage development rate and a significantly increased fatigue life when compared to the laminate with an identical stitch phase. Based on the micrographs, in-plane and out-of-plane waviness of axial fibres in the laminates were affected by the fabric shift. (Publication 3)

4) The performed compaction experiments revealed that the dry and wet compaction behaviour of a relatively thick quasi-UD preform was substantially affected by the stitch pattern but not by the stitch tension used in the non-crimped fabrics. The preform with a tricot stitch pattern compacted more effectively than the preforms with tricot-straight double and double

tricot stitch patterns. In addition, the fabric shift perpendicular to the axial fibre bundles (that is, whether the axial fibre bundles were overlapping or on top of each other) had a small but detectable effect on the thickness of the preform during dry and wet compaction experiments. Fibre volume fractions measured in wet compaction tests for laminates with different stitch patterns and tensions were close to the fibre volume fractions of the corresponding two-layer laminates used in the fatigue testing. (Publication 4)

1. Introduction

1.1 Quasi-unidirectional non-crimp fabrics

Quasi-unidirectional (quasi-UD) non-crimp fabrics (NCFs), a certain class of NCF textile reinforcements, have been developed to replace high-priced UD pre-pregs since they significantly reduce the cost associated with labour-intensive manufacturing and process time. Quasi-UD NCFs usually consist of two layers of unidirectional fibre bundles, as shown in Figure 1: the main layer is in the 0° direction, and there is a stabilizing layer formed from a small quantity of fibre bundles oriented at 90° (Vallons et al., 2013). The layers are joined together usually with a thin polyester stitch thread. Different stitch patterns and stitch tensions as well as stitch lengths and widths are used. Fibre bundles in stitched fabrics generally exhibit a very small amount of crimp, in which case the static properties (Bibo et al., 1997) and specifically the fatigue life of NCF reinforced laminates are better when compared to woven fabric reinforced laminates.
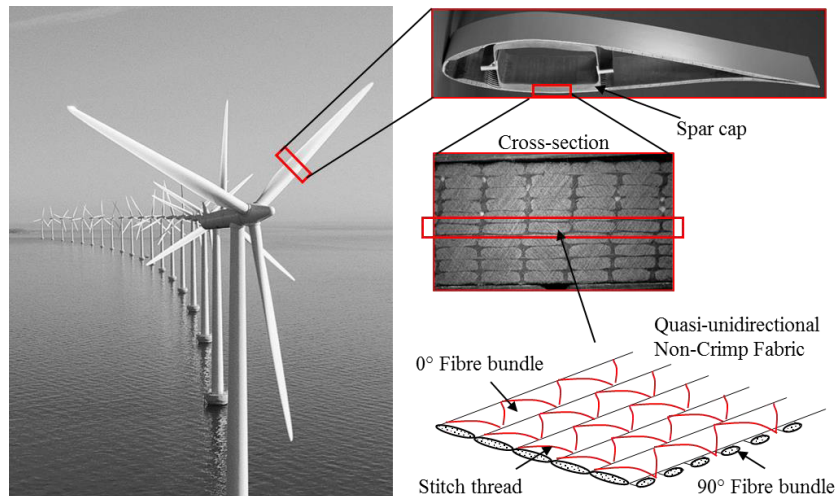

Figure 1. Quasi-UD Non-Crimp Fabric used in spar caps of wind turbine rotor blades.

Due to the good fatigue performance (fatigue life and *S-N* curve slope) and an inexpensive manufacturing process, the quasi-UD NCFs are widely used as a reinforcement in many structural applications that experience cyclic loading

during the service. For instance, they are the most commonly used reinforcements in the main load-carrying laminates, i.e., in spar caps (see Figure 1) of wind turbine rotor blades (Vallons et al., 2013; Zangenberg et al., 2014a). The blades undergo more than 10^8 load cycles during the typical 20-25 year service life of a wind turbine (Brøndsted et al., 2005; C. Kensche, 1996; C. W. Kensche, 2006; Vallons et al., 2013).

Although the fatigue life of quasi-UD NCF laminates is better when compared to woven fabric reinforced laminates, their fatigue performance is lower when compared to filament wound (Samborsky et al., 2012) and prepreg-based UD laminates. This is mainly due to the heterogeneity, i.e., due to internal structure variations in the mesoscale structure of the laminate, as shown in Figure 1 (cross-section). The internal structure variations partly result from artefacts caused by the stitching. In particular, stitching affects the waviness and cross-sectional shape of the fibre bundles in cross-ply and quadriaxial NCF reinforced laminates (Mattsson et al., 2007). Secondly, internal structure variations also depend on the mutual location of adjacent fabrics with respect to each other, i.e., whether the axial fibre bundles in neighbouring fabrics lie on top of each other or are overlapping. In addition, compressibility of a single NCF and a stack of NCFs during the laminate manufacturing process affects the thickness of the preform and thus the fibre volume fraction of the laminate. The fibre volume fraction also affects fatigue performance of the laminate (Carvelli and Lomov, 2015). Understanding the internal structure variation, e.g., the deformation and waviness of axial load-carrying fibre bundles on a mesoscale, may reveal how it affects fatigue damage evolution and performance of NCF reinforced laminates in load-carrying structures on a macroscale.

Experimental coupon level fatigue testing is problematic for quasi-UD laminates since standardised test specimens tend to fail prematurely at the end tabs (Mandell et al., 1992; Mandell et al., 1993; Nijssen, 2006; Zangenberg, 2013). Premature failure means that fatigue lives of the laminates are underestimated. Additionally, differences in fatigue damage evolution and performance of laminates with different internal structures (e.g., resulting from various UD fabric architectures) may not be found. To utilise the full potential of the laminates in cyclic-loaded structures and to be able to compare fatigue lives between different quasi-UD laminates, a test specimen configuration that fails in the gauge section and yields the true fatigue life for the laminate should be used in fatigue tests.

1.2 Scope and objectives

NCF reinforced composite structures are subjected to different types of fatigue loads during their service life. The loads are application specific and may include e.g. tensile, bending and torsion loads. This thesis focuses on tensile-tensile fatigue damage evolution and fatigue performance of quasi-UD GFRP laminates,

since tensile-tensile loading is the dominant fatigue loading type in many structures made of such laminates, e.g. in the spar caps of wind turbine rotor blades (Zangenberg, 2013).

The first aim of the thesis is to develop a test specimen configuration applicable for tensile-tensile fatigue testing of quasi-UD GFRP laminates. The specimen should fail in the gauge section, since commonly used standard rectangular test specimens tend to fail at the tabbed area. The thesis also aims to validate experimentally the performance of the developed specimen in fatigue testing of high-performance UD GFRP laminates made of powder-bound (non-stitched) NCFs.

The second aim is to find out how the stitch pattern and tension as well as fabric positioning (shifting) affect the tensile fatigue damage evolution and performance of quasi-UD NCF reinforced laminates. The stitch pattern and tension can be controlled and customised for a fabric and optimised to gain good fatigue performance. A non-controllable fabric shifting inevitably occurs during the lay-up phase of the laminate manufacture when the fabrics are stacked into a preform prior to impregnation. The fabric shifting affects the internal structure of the laminate and may result in a high scatter of fatigue test results.

The last part of the thesis concentrates on studying how the fibre volume fractions of thin test laminates correspond to the fibre volume fractions of relatively thick laminates needed in many applications such as the wind turbine rotor blades. Dry and wet compaction tests are performed to measure compressibility of thick preforms.

Specifically, this study answers the following questions:

- What is an applicable configuration for a test specimen intended for tensile-tensile fatigue testing of quasi-UD GFRP laminates?

- How do the stitch pattern and stitch tension of a quasi-UD NCF, and the fabric shift with respect to neighbouring fabrics, affect the internal structure variation of a quasi-UD NCF reinforced laminate, and specifically the axial load-carrying fibre waviness?

- How do the stitch pattern and stitch tension, and the fabric shift with respect to neighbouring fabrics, affect damage development and fatigue performance in tensile-tensile fatigue loading of quasi-UD NCF reinforced laminates?

- How do the stitch pattern and stitch tension, and the fabric shift with respect to neighbouring fabrics, affect the thickness of a thick preform during compaction and thus the final fibre volume fraction of a quasi-UD NCF reinforced laminate?

1.3   Dissertation structure

This thesis consists of four scientific research articles and a concluding summary. The first article (Publication 1) presents a dog-bone shaped test specimen configuration developed for tensile-tensile fatigue testing of quasi-UD GFRP laminates. It also provides a comparison of the fatigue lives measured for a high-performance UD GFRP laminate with a standardised rectangular test specimen and with two different dog-bone specimens. The developed dog-bone shaped specimen is utilised in the second article (Publication 2), which presents damage evolutions and measured fatigue lives for quasi-UD NCF reinforced laminates with different stitch patterns and stitch tensions. Fatigue damage evolutions and measured fatigue lives of quasi-UD NCF reinforced laminates with different fabric shifting cases are analysed in the third article (Publication 3). In addition, Publications 2 and 3 describe the measured internal structures of the prepared quasi-UD laminates and evaluate how the internal structure affects fatigue lives and damage evolution. Finally, the fourth article (Publication 4) presents the results of compaction tests performed for relatively thick quasi-UD preforms to study how well fibre volume fractions of thin laminates used in fatigue tests correspond to the fibre volume fractions of thick laminates.

The research work and its results are summarised in the following chapters. Chapter 2 presents the theoretical background of the work. Chapter 3 describes the materials used in experiments and essential research methods. The results are presented and discussed in Chapter 4. Finally, Chapter 5 concludes the main findings and gives recommendations for future research work.

2. Theoretical background

2.1 Fatigue testing of UD and quasi-UD laminates

Fatigue tests of composite laminates are commonly performed for test speci-
mens using a testing machine in a load-controlled mode by applying a sinusoi-
dal waveform. The testing machine counts the number of cycles (fatigue life)
that the specimen sustains before failure. The peak stress is simply calculated
by dividing the maximum load applied to the specimen by the initial cross-sec-
tion area of the gauge section. In this thesis, measured fatigue life denotes the
number of cycles that the specimen withstands until complete failure. If the
specimen prematurely fails outside the gauge section, i.e. at end tabs due to
stress concentration, the fatigue life of the laminate to be tested is underesti-
mated. Thus, the true fatigue life of the laminate is higher than the measured
fatigue life of the specimen. The true fatigue life of the laminate indicates the
life (cycles) that the specimen would withstand if the specimen would be opti-
mised and would have broken in the gauge section as desired.

Standardised fatigue test methods for UD GFRP laminates propose a rectan-
gular test specimen with end tabs, e.g. based on ISO standards (ISO 527-5,
2009), when tensile-tensile fatigue tests are performed in the main fibre direc-
tion. In the rectangular specimen, the highest stresses naturally occur at the re-
gion of the end tab junctions due to the shape of the specimen and test machine
clamping. Thus, damages typically initiate at the end tab junctions during cyclic
loading, and the specimens tend to fail at this region (Mandell et al., 1992; Man-
dell et al., 1993; Nijssen, 2006; Zangenberg, 2013). This type of failure might be
avoided by using proper tabs and adhesive and by controlling the grip pressure.
Nevertheless, failure initiation at the tab junctions indicates that cyclic stresses
in the end tab area are more detrimental than the stresses in the specimen's
gauge section. Consequently, the fatigue life of the studied laminate is underes-
timated. Moreover, due to the end tab failure, it is not possible to monitor dam-
age accumulation in the gauge section to the number of cycles that would result
in the laminate fatigue failure.

Rectangular specimens with straight end tabs are especially problematic in
tensile fatigue tests of quasi-UD laminates made of stitched fabrics. First, De
Baere et al. (2009) concluded that the highest stresses occur very locally in the

laminate end tab junctions based on their finite element (FE) simulations. Second, the internal structure of the laminates varies over a single stitch length in a quasi-UD NCF. Thus, there is a risk that internal structures of two different quasi-UD laminates are identical or very close to each other just at the stress-critical point at end tab junctions (at the point of highest stresses). Consequently, stresses at the critical points of the laminates may be close to each other, resulting in the specimens failing at the tabbed area and yielding comparable fatigue lives. Therefore, the effect of different fabric architectures, e.g. the effect of the stitch pattern and tension of quasi-UD NCFs on fatigue performance, may not be properly analysed when using rectangular specimens.

Waisted test specimens (dog-bone specimens) are often used in tensile fatigue testing of GFRP laminates. Dog-bone geometry is used to promote failure in the gauge section by decreasing the stress concentration at the tabbed area, i.e., by reducing the risk of failure in the tabs and gripping areas. However, this specimen shape may also be problematic, since UD and quasi-UD laminates have a tendency to split in the longitudinal direction from the edges of the curved area due to their low shear strength. Mandell and Samborsky (1997) have used dog-bone specimens in tensile fatigue tests of various GFRP laminates. They observed that the final failure mode was dependent on the relative amount of 0° fibres in the laminates. A large amount of fatigue test data for various UD GFRP laminates is available in the OptiDat database gathered by the wind turbine industry under the European OPTIMAT project (Nijssen, 2014). In this project, a dog-bone shaped specimen was occasionally used to prevent end tab failure – yet without a true success. Qian (2013) used a dog-bone geometry with tapered end tabs in fatigue tests of quasi-UD laminates, but unfortunately the specimens mostly failed at the end tabs. Aono et al. (2008) used a high curvature, double-notched specimen (notched in both thickness and width direction) to investigate fatigue damage development in quasi-UD NCF reinforced laminates. However, they did not report how the specimens failed. Zangenberg (2013) compared a long dog-bone specimen and the rectangular specimen (ISO 527-4) in tensile fatigue tests of quasi-UD NCF reinforced laminates by subjecting the specimens to only one stress level. Both the dog-bone and rectangular specimens failed outside the gauge section, but the dog-bone specimen yielded a slightly higher fatigue life.

2.2 Factors affecting fatigue performance of stitched NCF reinforced laminates

2.2.1 Fibre compaction and fibre volume fraction

Large composite parts reinforced with NCFs, such as wind turbine blades and boat hulls (Brouwer et al., 2003), are typically manufactured using a cost-efficient vacuum infusion (VI) process. The VI process is a liquid composite moulding process, and it normally contains four different stages: lay-up, pre-filling, filling, and post-filling (Govignon et al., 2008; Govignon et al., 2010; Govignon et al., 2013; Yang et al., 2012).

The lay-up stage involves the stacking of dry reinforcements, a peel ply, and a distribution medium on a solid mould. The stage also involves placing an inlet and vacuum tube at the mould and finally building a vacuum bag on the preform. The next stage is the pre-filling stage, which starts as the inlet tube is clamped and vacuum pressure is applied to the bag. During the pre-filling stage, the preform thickness changes depending on the reinforcements, applied vacuum, and time. The filling stage begins when the inlet tube is opened to saturate the preform with resin. Hammami and Williams et al. (2001; 1998) have found that the thickness of the preform reduces at a flow front depending on the lubrication effect of the resin and on fibre nesting. Finally, after the flow front reaches the vacuum tube, the inlet tube is typically clamped to start the post-filling stage. During the post-filling stage, excess resin flows from the mould cavity into the vacuum tube and the resin pressure begins to even out inside the vacuum bag. As a result, the thickness of the preform decreases. Several studies have been performed for various reinforcements to determine thickness changes along the preform during the pre-filling, filling, and post-filling stages of the vacuum infusion process (Govignon et al., 2013; Tackitt and Walsh, 2005; Yang et al., 2012; Yenilmez and Sozer, 2009; Yuexin et al., 2008).

The final thickness of the laminate partly depends on the compaction behaviour of the preform, which describes the ability of the reinforcement to be compacted perpendicular to the laminate plane. Hammami and Kelly et al. (2001; 2006) have found that the compaction behaviour depends on the structure of the reinforcement and on the lubrication, i.e., whether the fabric is dry or wet. Toll (1995; 1998) has proposed models to describe the behaviour of reinforcements under compressive loading. The final thickness of the laminate naturally affects the fibre volume fraction (Luo and Verpoest, 1999), which in turn affects the fatigue performance of the prepared laminate (Carvelli and Lomov, 2015). Dharan (1975a) has reported that an increase in the fibre volume fraction of "pure" UD GFRP laminates results in a steeper *S-N* curve slope. Mandell and Samborsky (1997) made a similar conclusion for quasi-UD NCF reinforced GFRP laminates.

2.2.2 Stitching

The fibre bundle stitching causes heterogeneity on a mesoscale in NCF reinforced laminates, which lowers fatigue performance of the laminates when compared to corresponding filament wound laminates (Samborsky et al., 2012) and laminates made of prepregs. For example, the stitching results in resin channels and openings in the NCFs since the stitching needles push aside fibre bundles (Vallons et al., 2013). The channels and openings are beneficial for the permeability of the fabrics (Vallons, 2009). Lundström (2000) has reported that even small variations in biaxial NCFs affect the permeability. Nordlund and Lundström (2005; 2006) developed a CFD model and found out that the width of the openings obviously affects the permeability of biaxial NCFs. Lekakou et

al. (2006) found out that the stitch pattern also affects the permeability of a bi-axial NCF. However, the channels and opening are also associated with the formation and propagation of damages during loading of the laminate (Truong et al., 2005).

Since the stitching needles push fibre bundles aside, they also cause minor fibre bundle waviness (Vallons et al., 2013). Mattsson et al. (2007) have reported that the stitching particularly affects the waviness and cross-sectional shape of fibre bundles in cross-ply and quadriaxial NCF reinforced laminates. Miller (1996) showed that the tow spacing and stitch density affect the waviness of bundles in biaxial and triaxial NCF reinforced laminates. Drapier and Wisnom (1999) found, via FE modelling, a clear relationship between the fibre waviness and compressive strength of biaxial NCF reinforced laminates. Tessitore and Riccio (2006) developed a novel FE model and concluded that fibre waviness decreased the tensile modulus of bi-axial NCF reinforced laminates. Various stitch patterns and tensions might also result in different levels of axial fibre bundle waviness for quasi-UD NCFs. For instance, a single stitch pattern that periodically zigzags around a bundle may result in higher in-plane waviness of the bundles when compared to the doubled stitching, which presumably keeps the fibre bundles better aligned.

The stitching also affects the formability and stability of the NCFs. Fabrics with a good drapeability and stability are relatively easy to handle and thus user-friendly (Vallons, 2009). Lekakou and Lomov (2006; 2011) have reported that the stitch pattern and tension particularly affect the formability and drapeability of the NCFs. For example, a loose stitch tension enables the fibres to move easily within stitch loops (S. Lomov, 2011), which means that the fibre bundles may spread more evenly in the laminate manufacturing process. In contrast, a loose stitch thread might enable the axial fibres to undulate or misalign easily when handling the fabrics prior to the laminate manufacturing. As a conclusion, the fibre waviness and the level of the permeability and formability can be adjusted by customising the stitching parameters. Verpoest and Lomov (2005) have reported on the textile modelling software WiseTex, developed in KU Leuven, in which the internal structure and deformability of textile fabrics (such as NCFs) can be analysed.

Many researchers have studied the effect of the presence of structural and non-structural stitching thread on the fatigue performance of NCF reinforced laminates. The term non-structural in this context refers to stitching that only joins the layer together, whereas structural stitching also reinforces the laminate in the thickness direction. The influence of a non-structural stitching thread on the tensile-tensile fatigue performance of quasi-UD GFRP laminates has been investigated by Mandell and Samborsky (1997), who found that removing the stitching from the quasi-UD NCFs prior to impregnation improved the fatigue life and lowered the slope of the fitted *S-N* curve. A similar tendency has been reported elsewhere (Aymerich et al., 2001; Aymerich et al., 2003;

Mouritz, 2004) for laminates, in which reinforcements were tied together with structural stitching. Mouritz (2004) found that structural stitching considerably lowered the fatigue performance of woven glass-fibre reinforced laminates. Aymerich et al. (2001; 2003) concluded that the fatigue performance of fibre-dominated [±45/0/90]$_S$ prepreg-based carbon-fibre reinforced laminates is reduced by structural edge-stitching, whereas the fatigue performance of matrix-dominated [±30/90]$_S$ laminates are considerably improved by structural edge-stitching. Carvelli et al. (2010) concluded that a structural stitch in a multi-ply carbon NCF composite with a stacking sequence of [45/-45/0/90/45/-45]$_S$ increases the fatigue life in the sewing direction of the structural stitch (0 direction) and reduces the fatigue life in the direction orthogonal to the sewing direction.

Based on the current literature, the presence of non-structural and structural stitching affects laminate fatigue performance considerably. Therefore, it can be expected that internal structure variations, depending on the stitching parameters, also affect the fatigue performance of NCF reinforced laminates. Only a few studies about the effect can be found in the current literature. Samborsky et al. (2012) compared the fatigue performance of four multi-directional NCF reinforced GFRP laminates being different only regarding the stitch type, but they did not observe any significant difference in the measured fatigue lives. Asp et al. (Asp et al., 2004) studied the effect of stitch pattern on the tensile-tensile fatigue performance of four different quasi-UD NCF reinforced carbon-fibre-reinforced laminates. They found only small differences between the fatigue lives and suggested that a high stitching density might lead to shorter fatigue life. Vallons et al. (2014) investigated the tensile fatigue performance of quasi-UD GFRP laminates having two slightly different tricot-straight double stitch patterns. They found only a very small difference between the laminate fatigue lives.

The stitch pattern and tension can have a significant effect on the internal structure and consequently on the fatigue damage evolution and performance of NCF reinforced GFRP laminates. Therefore, it is crucial to study how the stitch pattern and tension particularly affect the axial load-carrying fibre waviness, since wavy fibres tend to straighten in tensile loading, resulting in fibre-matrix debonding and matrix damage (Piggott, 2002). Edgren et al. (2004) studied the formation of damage in a bi-axial NCF reinforced carbon-fibre laminate during quasi-static tensile tests. They found that transverse cracks occurred first, but they also observed longitudinal cracks. They further analysed the laminate behaviour with an FE model to find out the level of stress concentrations caused by the longitudinal fibre waviness. Although the effect of stitch pattern on the fatigue performance of quasi-UD laminates has also been investigated (Asp et al., 2004; Vallons et al., 2014), there is still a lack of detailed information about the effects of stitch pattern and tension on the internal structure, fatigue damage evolution and performance of quasi-UD laminates in the current literature. Finding an optimal stitch configuration regarding fatigue necessitates characterisation of the stitching-related artefacts in the laminate.

2.2.3 Fabric shifting with respect to neighbouring fabrics

A fabric shift in relation to neighbouring fabrics inevitably occurs during a true-life lay-up stage of the VI process. Fabric shifting perpendicular to the axial fibre bundles may occur, in which case the axial bundles in fabric layers may lie on top of each other or they can be overlapping (in other words, nesting), as schematically illustrated in Figure 2. When the bundles lie on top of each other, resin-rich areas (resin channels) form throughout the laminate thickness. When the bundles overlap, they are partly pressed between each other in the neighbouring fabric layers, and the resin-rich areas are smaller. The internal structures of the laminates are thus different. Fang et al. (2014; 2015) have shown that the mutual locations of upper and lower fabrics of 0°/90° NCFs and the mutual locations of adjacent axial bundles in UD fabrics also greatly affect the out-of-plane permeability of the preforms.

a)   b)

Figure 2. Schematic cross-sectional view of a UD preform when axial fibre bundles are located: a) on top of each other, and b) overlapping.

Fabric shifting parallel to the axial fibre bundles can also occur during stacking of the fabrics. When a stitched fabric moves parallel to the axial fibre bundles in relation to the neighbouring fabric, the stitch phase varies between the fabrics. The stitch phase is in extreme cases identical or reversed between the fabrics, as illustrated in Figure 3a and 3b. The internal structure of a laminate is naturally dependent on the stitch-phase difference due to the stitching induced fibre (and fibre bundle) waviness of NCFs. Lomov et al. (2003) have studied how the stitch-phase difference affects layer thickness in UD NCF reinforced laminates. Their Monte Carlo simulation revealed that when the stitching travels in the same phase in adjacent layers, the thickness per layer is slightly higher than in the case when the stitching does not coincide in adjacent layers.
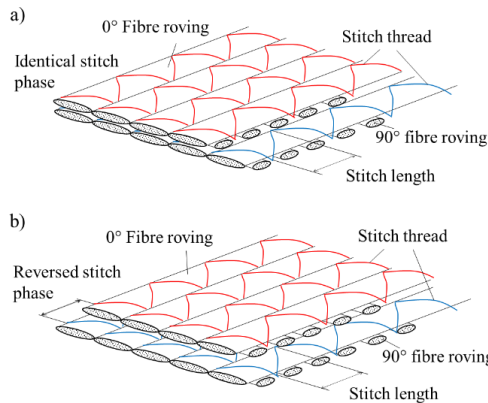
Figure 3. Two quasi-UD non-crimp fabrics having a) an identical stitch phase and b) a reversed stitch phase between the fabrics.

Control of the fabric shift is normally impossible in the manufacture of composite parts. However, it is important to know over which range fabric shifting influences fatigue performance so that stitch parameter based variations can be reliably measured. To be noted is that there are also other reasons for the fatigue life scatter of laminates, e.g., variations in fibre and fabric properties, variations in laminate manufacturing methods which often cause a large number of defects (Vassilopoulos and Keller, 2011), and variations in test conditions (Nijssen, 2006). These variations should be minimised when stitch parameter and fabric shift based effects on fatigue life are being measured.

3. Materials and methods

This section provides a brief description of materials and research methods used in the thesis. The individual publications (Publications 1–4) of the thesis provide detailed descriptions of the applied materials and methods.

3.1 Materials

In Publication 1, the studied reinforcements were a newly developed UD powder-bound fabric and a quasi-UD stitched NCF. The UD powder-bound fabric consisted of 1152 g/m² continuous glass fibres in the 0° direction, 25 g/m² thermoplastic powder binder and 4 g/m² of synthetic monofilaments. Its total areal weight was 1181 g/m². The quasi-UD NCF consisted of 1152 g/m² continuous glass fibres in the 0° direction, 36 g/m² of glass in the 90° direction and 12 g/m² of polyester stitch thread with the tricot stitch pattern and normal stitch tension.

In Publications 2-4, the studied quasi-UD stitched NCFs consisted of continuous glass rovings (bundles) in the 0° direction and continuous stabilizing glass yarns (bundles) in the 90° direction. The NCFs differed in terms of stitch pattern and stitch tension, and in some tests in terms of the glass fibre manufacturer (considered later as fibre type). The studied stitches were tricot, double tricot, and tricot-straight double patterns, as illustrated with red lines in Figure 4. The fabrics stitched with the double tricot stitch pattern were manufactured both with a low and high stitch tension. The stitch width and length were equal in all fabrics. The total areal weight of the fabrics was close to 1000 g/m², including 946 g/m² of glass in the 0° direction, 40 g/m² of glass in the 90° direction and 15-30 g/m² of polyester stitch thread. Variation in material properties was minimised by manufacturing the test reinforcements specifically for the study from the same batches of glass roving. For the same reason, all test laminates were manufactured from the same batches of the epoxy resin (EPIKOTE RIMR135) and hardener (RIMH137).
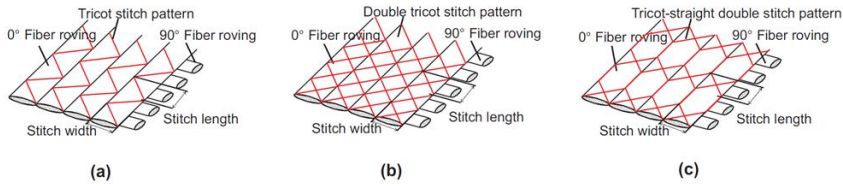
Figure 4. Schematic view of used quasi-unidirectional stitched non-crimp fabrics with a) a tricot, b) a double tricot, and c) a tricot-straight double stitch pattern.

3.2 Laminate preparation

All test laminates were prepared with the vacuum infusion (VI) method. In Publication 1, UD and quasi-UD laminates with a stacking sequence of $[0°]_2$ were prepared between two heated glass plates. In Publications 2 and 3, quasi-UD laminates were prepared using the method called resin infusion under flexible tooling (RIFT II) (Summerscales and Searle, 2005), i.e., by using a flat mould and a plastic vacuum bag. The fabrics were stacked with an orientation of $[0°]_2$. The lay-up was slightly unsymmetrical, that is, the stabilizing 90° yarns were on the bottom side, since the fabrics are normally stacked in this way in the manufacture of composite parts.

In Publication 3, four different fabric shift cases were studied, as illustrated in Figure 5a-d. With Case 1 (Figure 5a), the fabrics were placed so that the axial fibre bundles were precisely located on top of each other and the stitch phase was adjusted to make it identical between the fabrics. With Case 2 (Figure 5b), the fabrics were placed so that the axial fibre bundles were overlapping and the stitch phase was adjusted to make it identical between the fabrics. With Case 3 (Figure 5c), the fabrics were placed so that the axial fibre bundles were located on top of each other and the upper fabric was shifted one stitch length parallel to the axial fibre direction. With Case 4 (Figure 5d), the fabrics were placed so that the axial fibre bundles were overlapping and the upper fabric was shifted one stitch length parallel to the axial fibre direction.
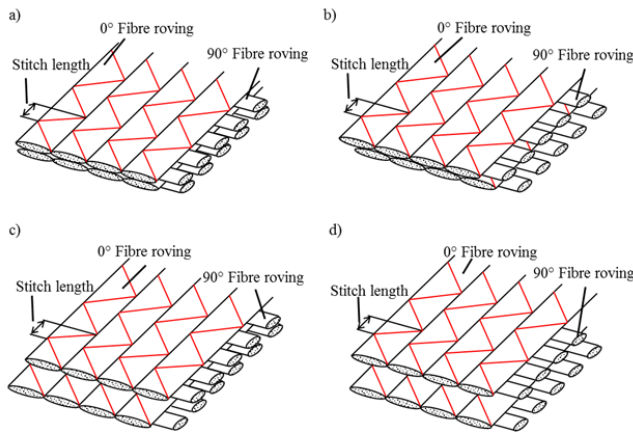

Figure 5. Schematic illustration of four different lay-up cases.

3.3   Geometry and preparation of fatigue test specimens

In Publication 1, a well-known and commonly used rectangular specimen according to the ISO 527-5 standard (ISO 527-5, 2009) was used as a reference specimen in fatigue tests. As a relatively high stress concentration exists at the end tab area due to the shape of the rectangular specimen and the specimen clamping, test specimen development was focused on waisted (dog-bone shaped) specimens to decrease the stress concentration at the tabbed area and to keep shear stresses low at the edges of the specimen.

Two slightly different dog-bone shaped specimens with low levels of curvatures, A and B (Figure 6), were selected for the test program in Publication 1. Specimen A (Figure 6b) is based on a previous investigation (Zangenberg, 2013), in which the dog-bone specimen has been found to yield higher fatigue lives for a quasi-UD GFRP laminate than the rectangular specimen. The geometry of the specimen B (Figure 6c) was developed from the geometry of the specimen A with an aim to find a specimen with lower stress concentrations at the tab area in tension loading. The geometry is a result of several FE analyses and fatigue tests conducted by the author with different specimen curvatures, spacings of the end tabs and taper angles of the end tabs. Specimen B differed in geometry from the specimen A in terms of lower curvature, longer tab tapering and shorter spacing of the end tabs.
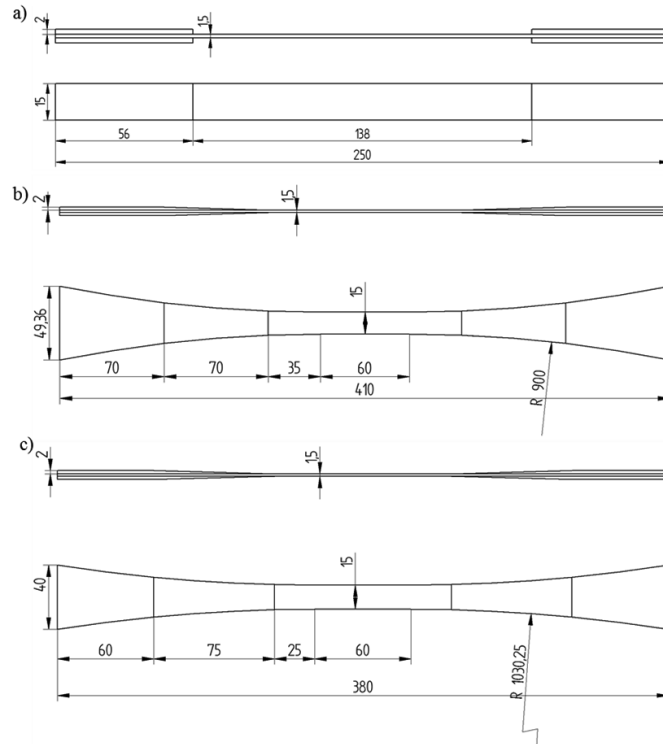

Figure 6. Dimensions of a) ISO 527-5:2009, b) dog-bone A (Zangenberg, 2013) and c) dog-bone B test specimens.

In addition to geometry differences, different end tab laminates, tab bonding adhesives and manufacturing processes were used in the manufacture of the dog-bone A and B specimens. The differences are summarised in Table 1.

Table 1. End tab laminates, used adhesives for end tab bonding and manufacturing processes used in the manufacture of dog-bone A and B specimens.

	Dog-bone A	Dog-bone B
End tab laminate	Ten plain weave fabrics (230 g/m^2) and high glass-transition temperature epoxy resin.	Nine uniform twill weave layers (290 g/m^2) and Araldite/Aradur 5052 epoxy resin system.
Adhesive	Epoxy adhesive (3M, DP460)	Epoxy adhesive (3M, DP190)
Specimen manufacture	Tab laminate sections blasted with glass particles and machined to the required tapering angle. The end tab sections cleaned with ethanol prior to bonding. The prepared end tab sections bonded, fixed and pressurised with clamps to the test laminate and cured for 16-24 hours at 40 °C.	End tab and test laminate surfaces grit-blasted with aluminium oxide and cleaned with methyl ethyl ketone. A thin nylon scrim cloth layer used in the bond line to control the adhesive layer thickness. The specimens cured in room temperature for 24 hours under 0.8 bar vacuum pressure in a vacuum bag and later post-cured at 45 °C for 2 days. Finally, tab taper ground and laminate-end tab junctions manually smoothed with sandpaper.

3.4 Finite element analysis

Finite element (FE) analysis is a method applied to various engineering studies to find approximate solutions for boundary value problems. In Publication 1, Abaqus™/Standard v6.14-1 software was used to evaluate stress states in three different specimens and to explain reasons for the identified failure modes and measured fatigue performances of the specimens. Specimens made of a quasi-UD GFRP laminate were modelled for the analyses since such laminates were studied in almost all subsequent fatigue tests of the thesis. The thickness of the test laminate was set to 1.5 mm, representing a laminate manufactured from two quasi-UD NCFs with a stacking sequence of $[0°]_2$. A woven-fabric epoxy laminate with the thickness of 2 mm and with layer orientations of ±45° was used as the tab material. To keep the model simple, the effect of the gripping pressure and adhesive layers between the tabs and laminate were ignored. Only half of a specimen was modelled to reduce the calculation time. The interaction between the test laminate and the end tabs was modelled by using a tie constraint with surface-to-surface discretization. The specimen models were meshed with a mesh size of approximately 1 mm, using C3D20R quadratic brick elements with reduced integration. Finer mesh (≈0.5 mm element size) was used at an area close to the tab edges for the rectangular specimens where higher

stress concentrations were expected due to the specimen geometry (sharp edge of the end tabs). The element behaves very well and is an excellent general purpose element. A longitudinal stress ($\sigma_{applied}$) of 600 MPa was applied to the gauge section. The absolute value of this stress is, however, not important since the simulation was linear-elastic and the width of the gauge section was the same in all specimens. The stress concentration factor SCF = max $\{\sigma_{11}/\sigma_{applied}\}$ was computed along the specimen length and compared between the different specimen geometries. A limitation of the applied linear-elastic analysis is that it does not consider the damage initiation and evolution during loading.

3.5   Internal structure characterisation

The internal structure of the quasi-UD laminates was characterised using cross-sectional microscope imaging. In Publications 2 and 3, heights and widths of the axial fibre bundles (dimensions *a* and *b* in Figure 7a), distances between the laminate mould surface and the upper fibre bundle bottom (dimension *c* in Figure 7a), and widths of the resin channels (dimension *d* in Figure 7a) were measured, based on microscope images acquired in five equidistant cross-sections within consecutive stitch loops (Figure 7a).
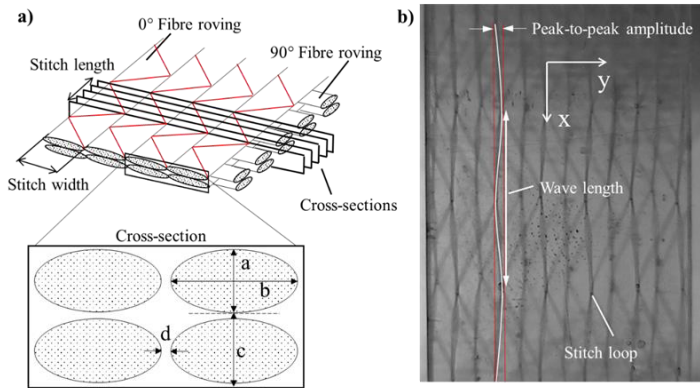
Figure 7. a) Illustration of a test laminate and its cross-section and b) an in-plane image of the test laminate surface.

   In Publications 2 and 3, the in-plane and out-of-plane waviness of axial fibres were seen to be important geometry parameters affecting fatigue performance of quasi-UD laminates. Out-of-plane fibre misalignment angles of axial fibres were estimated from measured distances between the laminate mould surface and the upper fibre bundle bottom (dimension *c* in Figure 6a). The highest misalignment angles were determined by taking the highest measured distance difference in between two adjacent cross-sections and by assuming a constant fibre angle in between the cross-sections. The in-plane waviness of axial fibre bundles was determined based on the photographs of the laminate surface (see Figure 7b). The peak-to-peak amplitude and distance between the stitch loops were measured from the upper fabrics since the axial fibre bundles and stitch loops of this layer were clearly visible in the photographs. The in-plane waviness of

the bundles was presumed to be of sine form. Thus, the calculated maximum slope of the tangent, i.e. the maximum in-plane misalignment of the fibre bundle, is:

$$y'(x)_{max} = \frac{2\pi \cdot A}{\lambda} \tag{1}$$

where A is the amplitude and λ is the wavelength.

The mutual location of the axial fibre bundles in the laminates (lay-up cases in Figure 5) was determined visually from the cross-sectional microscope images. The mutual location of the stitching in the laminates was determined visually from the photographs of the laminate surface (see Figure 7b).

3.6   Tensile-tensile fatigue tests

Fatigue testing is a test method to determine the material capability of withstanding a cyclic load (stress) applied to the material. Basic fatigue testing involves the preparation of test specimens and the tests where the specimens are subjected to a cyclic loading and loaded until failure. In Publications 1-3, a hydraulic testing machine with a 100 kN load cell was used for tensile-tensile fatigue testing with a stress ratio $R=0.1$ (ratio of the applied minimum and maximum stress within a cycle). The tests were performed in a load-controlled mode and by applying a sinusoidal waveform. Each fatigue test was continued until the complete failure of the specimen (separation into two parts).

Fatigue data was presented in a conventional linear-logarithmic graph (applied peak stress versus cycles to failure), which is generally referred to as the material's *S-N* curve. The relationship between the applied maximum stress (peak stress) and the number of cycles to failure was used with the power-law model (Basquin 1910) to analyse the fatigue data:

$$N = C \cdot S^m \tag{2}$$

In Eq. (2), S is the maximum applied stress, C is the intercept parameter, N is the measured fatigue life and m is the slope of the *S-N* curve. The least-squares regression method was used to obtain the values of the parameters C and m according to the ASTM E 739 standard, using the number of cycles as a dependent variable and the stress as an independent variable (ASTM E739-91, 2004). The coefficient of determination R^2 was defined for each data set to indicate how well the *S-N* data fits the curve.

In Publication 1, stiffness degradation was measured for the UD powder-bound fabric reinforced laminate in the gauge section of some dog-bone A and B specimens to see whether or not the stiffness decreases during a fatigue test. The longitudinal strain was measured continuously during the fatigue test in the specimens' gauge section using two back-to-back mounted extensometers with a gauge length of 50 mm. Also, the distance between the upper and lower grips was measured and recorded during the tests. The stiffness in the gauge section

was calculated for each fatigue cycle as the slope of the full hysteresis loop, i.e., the stiffness was defined as the ratio of the laminate fatigue stress and strain range. The overall stiffness between the grips was calculated as the ratio of the applied load and displacement range from the displacement-load hysteresis loop.

3.7 Damage monitoring using photography

The damage initiation and progression in the specimen's gauge section were monitored visually and recorded during the fatigue tests by photography. Digital images were taken for pristine specimens, after the quasi-static tests, and also during the fatigue tests after 1000, 5000 and 10 000 cycles and later usually after intervals of 10 000 cycles. Especially for the GFRP laminates used in this thesis, the gauge sections of the specimens were extraordinarily transparent due to the very smooth surfaces of the test laminates and the very transparent nature of the matrix and glass fibres. Individual glass fibres were not visible, but the stitch threads in stitched NCF reinforced laminates and synthetic monofilaments in UD non-stitched laminates remained visible. Therefore, matrix cracks or fibre-matrix debonds and voids were easily detectable with an auxiliary light. The type of crack, i.e. whether it was a matrix crack or fibre/matrix debond, could not be identified from the images. Therefore, the term crack is later used to refer to matrix cracks, fibre/matrix debonds, and their possible combinations.

3.8 Compaction experiments

The compressibility of a relatively thick preform was determined by measuring the thickness of the preform during the VI process. In Publication 4, the compaction during the pre-filling (dry compaction), filling and post-filling stage (wet compaction) was measured using the in-house developed experimental set-up shown in Figure 8. The set-up consisted of an integrally heated mould, an in-house-developed movable supporting framework with displacement sensors, a data acquisition system, a vacuum pump, and a vacuum sensor.

In dry compaction tests, step compaction was performed, i.e. vacuum pressure was increased stepwise with an interval of 0.1 bar from the initial 0 bar to 0.9 bar, with a dwell time of one minute between each step. In wet compaction tests, resin was infused to the preform using 0.9 bar vacuum pressure. Thickness evolution was recorded continuously during the compaction tests. The measured thickness comprises the thickness of the preform and the vacuum bag in the dry compaction tests, and the thickness of the preform, peel ply, distribution medium and vacuum bag in the wet compaction tests.
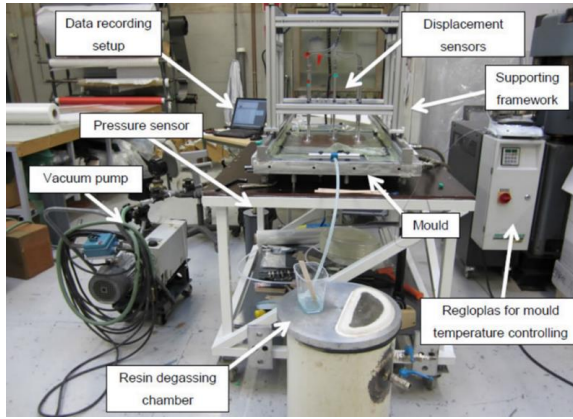
Figure 8. Experimental set-up used in compaction tests.

The fibre volume fraction of an impregnated preform (after wet test) was estimated with the following equation (Curtis, 1988):

$$V_f = \frac{A_w n}{\rho_f h} \tag{3}$$

where A_w is the areal weight of one fabric layer, n is the number of layers, ρ_f is the density of the fibre, and h is the thickness of the preform under compaction. The thickness of the preform used in FVF calculations is the measured thickness minus the thickness of the peel ply, distribution medium, and vacuum bag. Total thickness of the peel ply, distribution medium, and vacuum bag after removing them from a post-cured specimen was measured to be 0.907 ± 0.012 mm (average ± standard deviation). A possible thickness change of the peel ply, distribution medium, and vacuum bag during the compaction was not considered.

3.9 Statistical analyses

Statistical analysis is a research methodology to study the collection, analysis, interpretation, presentation, and organization of data. In Publications 1-3, a specified regression with fatigue life data analysis was performed with the aid of the MINITAB program to statistically compare the significance of the difference in fatigue lives between the test laminates (*Minitab 17, 2014*). In addition, a two-sample student's t-test was used in Publication 2 for characterising the difference in average values of internal structure parameters between the quasi-UD laminates with high and low stitch tension. In both analyses, the probability that there is no difference in the studied parameters between two laminates is indicated by the *p*-value. A 95% confidence level (significance level α = 0.05) was used to define the difference between the laminates, that is, if *p* is smaller than 0.05, there is a significant difference in the studied parameters.

4. Results and Discussion

4.1 Development of a test specimen for tensile fatigue tests (P1)

The main objective of the first research phase (Publication 1) was to develop a test specimen configuration that would fail in the gauge section in tensile-tensile fatigue tests of quasi-UD GFRP laminates. Another objective was to measure fatigue performance of a UD GFRP laminate reinforced with a newly developed powder-bound fabric and to compare it against the performance of a quasi-UD GFRP laminate reinforced with a conventional stitched fabric.

4.1.1 Influence of specimen geometry on stress distributions

The stress distributions of the rectangular specimen (Figure 9 a-c) indicated that laminate stresses are highest in a small local region at the end of the tabs. A calculated SCF of 1.32 was found at the end of the tabs (Figure 9a and Figure 12). The SCF is very high and agrees with the value given by De Baere et al. (2009), who calculated the SCF of 1.28 under the tabs of a rectangular specimen made of a carbon-fibre reinforced laminate.
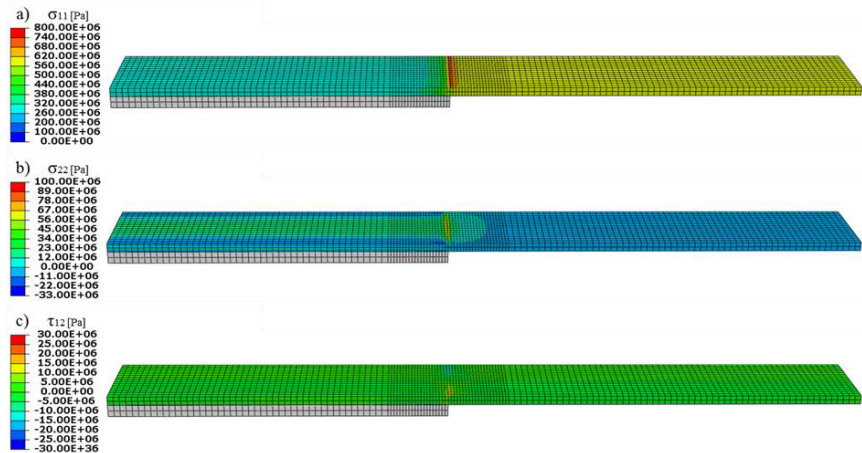
Figure 9. a) Longitudinal, b) transverse and c) shear stress distributions in the rectangular specimen (ISO-527-5). Upper end tab is ignored in the figures, and the lower end tab is displayed in white.
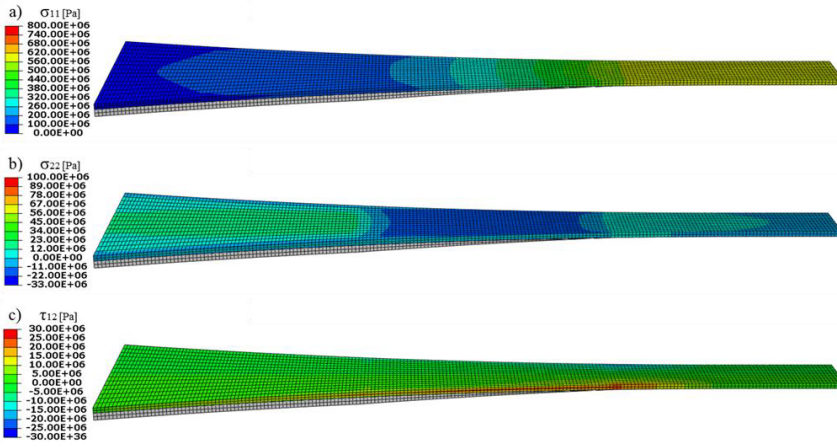
Figure 10. a) Longitudinal, b) transverse and c) shear stress distributions in the dog-bone A specimen (ISO-527-5). Upper end tab is ignored in the figures, and the lower end tab is displayed in white.
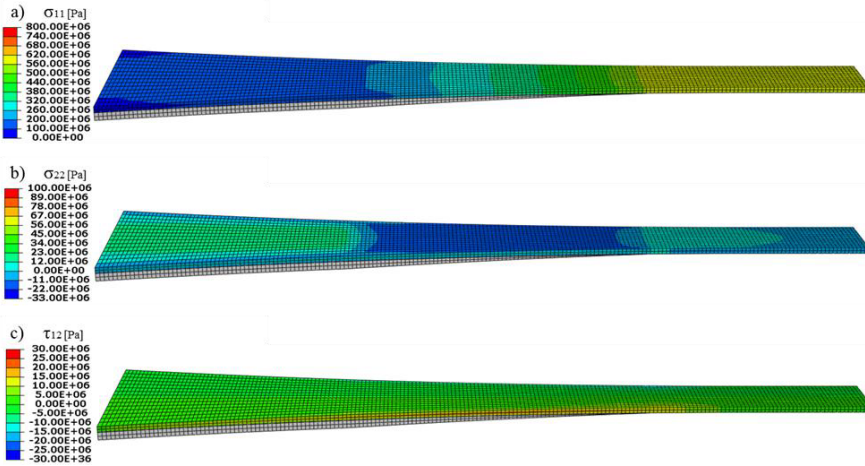
Figure 11. a) Longitudinal, b) transverse and c) shear stress distributions in the dog-bone B specimen (ISO-527-5). Upper end tab is ignored in the figures, and the lower end tab is displayed in white.
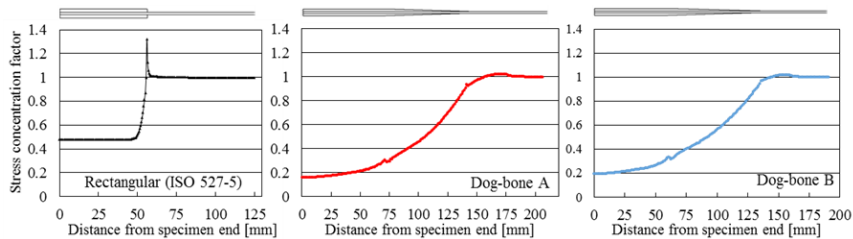
Figure 12. Stress concentration factor along the rectangular and dog-bone specimens from the end of the specimens.

The SCF of 1.02 was calculated for the dog-bone A and B specimens at the point (node value) where the curvature begins outside the tabbed area (Figure 10a, Figure 11a and Figure 12). The SCF of the dog-bone specimens is thus

clearly lower compared to the SCF of the rectangular specimen. The mesh (element size ≈1 mm) was fine enough with the dog-bone specimens since the stresses practically did not change with a finer mesh due to the smooth geometry of the specimens.

The highest shear stress of 28.8 MPa located at the edge of the end tab in the rectangular specimen. The highest shear stress of 24.9 MPa located at the edges next to the tab-laminate intersection in the dog-bone A specimen. In the dog-bone B specimen, the highest shear stress of 21.6 MPa located at the edges of the test laminate under the end tabs. The highest shear stress of the specimen A is 15% higher than the highest shear stress value of the specimen B. Samborsky et al. (2012) reported that the shear strength of a quasi-UD GFRP laminate is roughly 55 MPa. The highest shear stresses of both dog-bone specimens were below the shear strength of the laminate. However, the highest shear stress of the specimen A is closer to the shear strength of the laminate, indicating faster edge splitting during the fatigue tests.

Based on the FE analyses, the SCFs were substantially lower for the dog-bone specimens when compared to the rectangular specimen. In addition, small changes in the dog-bone geometry had a clear effect on the maximum shear stress value at the edges of the specimen and on the area with high shear stress. Apparently, the lower curvature of the dog-bone B specimen was the main reason for the decreased maximum shear stress and for the decreased area of high shear stress. A low shear stress reduces edge splitting and further reduces the risk of delamination between the tabs and the laminate. Even though the mesh was fine enough for the dog-bone specimens, that is, the stress values did not change in practice with a finer mesh, the selection of an element type and integration points in the elements may affect the absolute stress values. However, similar element types were used for each specimen so that possible error from absolute stress values (true values) would be close to the same with each specimen. The performed elastic analyses naturally give only an initial understanding of the stress distribution and a hypothesis of the failure zone. The evolution of the damage with different damage modes creates a redistribution of the stress and possibly a different failure zone. It should also be noted that stress components were compared separately between the specimens. A suitable stress criterion might reveal even better differences between the specimens.

4.1.2 Fatigue damage evolution in UD laminates

Tensile-tensile fatigue tests of UD laminates were performed by monitoring damage evolution during the tests to see whether the damages initiate and propagate in the gauge section and to find out in which location the specimens finally break. Each rectangular specimen finally failed at the end tabs (Figure 13a). No significant damage, i.e. matrix cracks, axial cracking or fibre breakage, was detected in the gauge section. Thus, it is obvious that the specimens failed at the tabs due to the high stress concentration (see Section 4.1.1).

During the fatigue tests of dog-bone A specimens, very small matrix cracks initiated in the gauge section of the specimen and longitudinal splitting initiated at curved free edges of the specimen and propagated along the axial fibres towards the test machine grips, resulting in delamination or detachment between the laminate and the end tab. It was difficult to judge whether the damage occurred in the adhesive layer or in the laminate-adhesive interface, since several fibres from the UD laminate were stuck on the adhesive in detached tabs. Finally, the specimens failed at the end tabs, as shown in Figure 13b.

Some dog-bone B specimens failed similarly to the dog-bone A specimens, but several specimens seemed to fail in the gauge section (Figure 13c), albeit some of them also experienced edge splitting and delamination at the tabbed area. In the specimens that failed in the gauge section, matrix cracks were observed throughout the gauge section with severe damages such as some axial cracks and several fibre breakages which usually initiated at the points where single synthetic monofilaments were located.

Based on the analysis and test results, it can be concluded that lower shear stresses in the dog-bone B specimen at least delayed the edge splitting (highest shear stress of the specimen A is 15% higher than the highest shear stress value of the specimen B). The other differences (end tab material, adhesive and manufacturing procedure) of the dog-bone A and B specimens may further have delayed delamination and/or end tab detachment in the dog-bone B specimen so that the damages had more time to develop in the gauge section. If the same end tabs, adhesive and manufacturing procedure had been used for both dog-bone specimens, a proper proof of the different behaviour would have been provided.

In the current literature, the progressive damage development in fatigue tests of UD GFRP laminates has been observed to initiate by matrix cracking, which is followed by axial fibre failures and fibre-matrix interface failures (or just axial cracks) (Curtis, 1991; Dharan, 1975a; Dharan, 1975b; Gamstedt et al., 1999). Here, the severe damage initiation points in the gauge section apparently contained small defects, e.g., local fibre undulation or misalignment, or local manufacturing defects such as small voids. Consequently, these points were the weakest in terms of fatigue and led to damage initiation and progressive damage accumulation. The damages (axial splitting and delamination) propagated in the axial direction towards the end tabs, which caused the final failure of the specimen either in the gauge section or at the end tab area. The specimens that failed in the end tabs had usually delaminated between the tabs and the laminate before the damages initiated from the gauge section reached the end tab area.
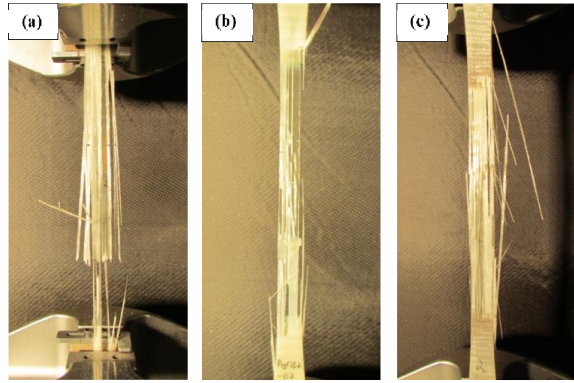
Figure 13. Typical examples of failed a) rectangular, b) dog-bone A and c) dog-bone B test specimens at the end of the tensile fatigue test; UD powder-bound fabric reinforced laminate.

4.1.3   Fatigue damage evolution in quasi-UD laminates

Tensile-tensile fatigue tests were further performed for quasi-UD laminates reinforced with a stitched fabric. Rectangular and dog-bone B specimens were used in these tests.

In the rectangular specimens, transverse cracks in the backing fibre bundles and a few small axial cracks in the axial fibre bundles developed in the gauge section. However, all rectangular specimens finally failed close to the end tab area, as shown in Figure 14a. The reason for the failure was obviously a high stress concentration in that area. The observed damages in the gauge section are in line with the results provided by the current literature, since many researchers have reported that transverse cracks initiate in the backing bundles in quasi-UD GFRP reinforced NCF laminates during tensile fatigue loading (Jespersen et al., 2015; Jespersen et al., 2016; Zangenberg et al., 2014b).

The dog-bone B specimens experienced damages such as transverse matrix cracks, axial cracks and fibre breakages in the gauge section (see Figure 15). The specimens seemed to fail frequently in the gauge section, as shown in Figure 14b. Thus, the damages had enough time (cycles) to initiate and propagate in the gauge section of the dog-bone B specimens before the damages in the tabbed area would have broken the specimens. Clearly, stress concentrations outside the gauge section of the dog-bone B specimen are not so detrimental in fatigue testing of quasi-UD laminates. The internal structure of the laminate, e.g. transverse bundles and fibre waviness, may cause even higher stress concentrations in the gauge section of the laminates. As a result, damages initiate in the gauge section and lead to the progressive damage evolution.
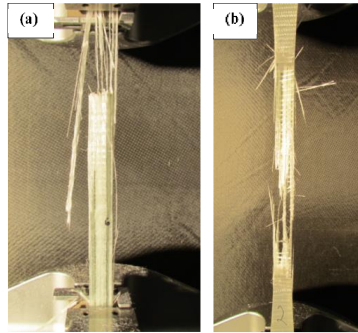
Figure 14. Typical examples of failed a) rectangular and b) dog-bone B specimens after the tensile fatigue test; quasi-UD stitched fabric reinforced laminate.
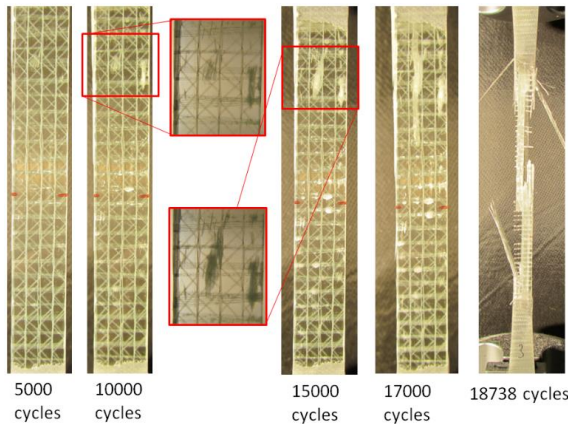
Figure 15. Typical damage initiation and development in the quasi-UD stitched fabric reinforced laminate during the tensile fatigue test of the dog-bone B specimen.

4.1.4 Stiffness degradation in UD laminates

Composite materials normally undergo stiffness degradation in fatigue loading resulting from progressive damage accumulation (Harris, 2003; Vassilopoulos and Keller, 2011). Stiffness degradation was measured for the UD powder-bound fabric reinforced laminate in the gauge section of some dog-bone A and B specimens.

Normalised stiffness degradation curves (dashed curves) in Figure 16a reveal that stiffness degradation did not occur in the gauge section of the dog-bone A specimens. The solid curves indicate that stiffness degraded between the upper and lower grips, meaning that damages (or slippage) occurred outside the gauge section, i.e. in the tabbed area. The fall of some dashed curves in Figure 16b indicates that some dog-bone B specimens experienced stiffness degradation in the gauge section, while the overall stiffness (solid curves) remained almost constant until the final failure. The stiffness loss in the gauge section supports the observed damage evolution in the gauge section during the fatigue test.
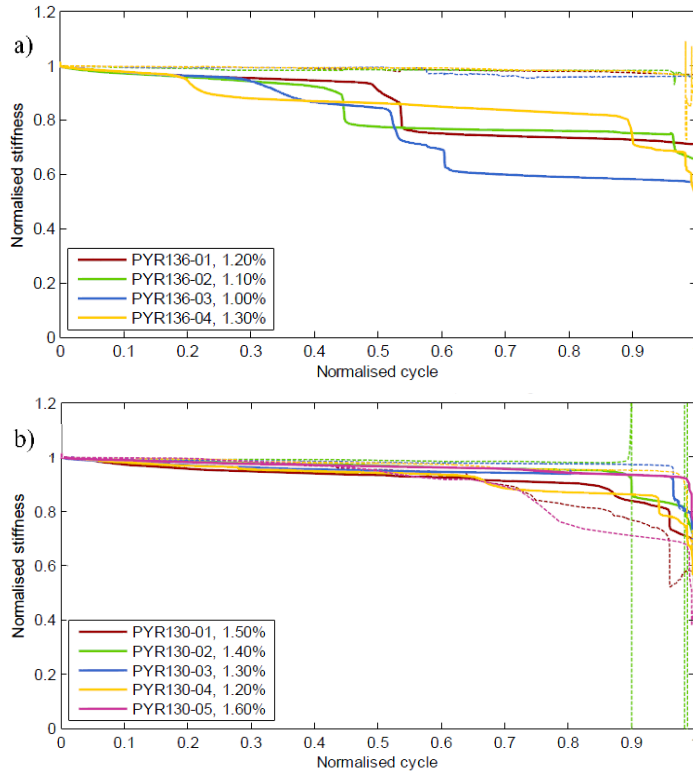
Figure 16. Normalised stiffness degradation curves of a) dog-bone A and b) dog-bone B speci-
mens during the fatigue tests. Dashed lines denote the average normalised stiffness degra-
dation in the gauge section, and solid lines imply normalised stiffness degradation of the
entire specimen measured between the lower and upper grips.

4.1.5 Tensile-tensile fatigue performance of the laminates

To compare measured fatigue lives of the UD powder-bound fabric reinforced
laminate between the different test specimen configurations, the fatigue test re-
sults were plotted in a conventional stress-lifetime graph. *S-N* curves calculated
with Equation 2 and the corresponding 95% confidence bands in Figure 17 in-
dicate that the specimen geometry had a significant influence on the measured
fatigue lives. The fatigue lives measured with the dog-bone B specimen were
over nine-fold when compared to the fatigue lives measured with the rectangu-
lar test specimen, and over three-fold when compared to the fatigue lives meas-
ured with the dog-bone A test specimen. The results mean that the fatigue lives
measured with the dog-bone B specimen are much closer to the true fatigue lives
of the laminate. Lower shear stresses in the dog-bone B specimen at least de-
layed edge splitting. Presumably, the combination of different end tab materi-
als, adhesives and manufacturing procedures of the dog-bone B specimens also
delayed damages in the tabbed area, resulting in higher fatigue lives for the dog-
bone B specimens. It seems that small differences between the specimens sig-
nificantly affect the fatigue performance. However, the failure of some dog-bone
B specimens at the tab area indicates that there is still a need to further develop
the specimen.

Figure 17. *S-N* curves with corresponding 95% confidence bands for the UD powder-bound fabric reinforced laminate, measured with the rectangular and dog-bone test specimens.

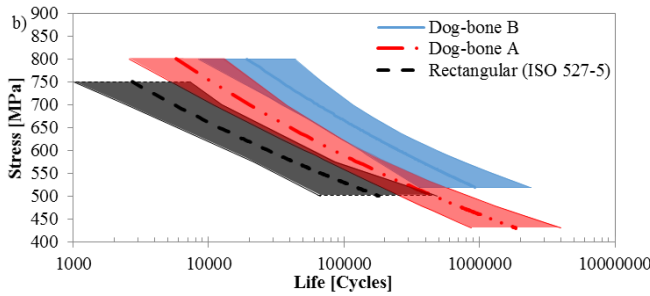*S-N* fatigue results of the quasi-UD stitched fabric reinforced laminate, measured with the rectangular and dog-bone B specimens (Figure 18), also show that fatigue lives measured with the specimens are significantly different, i.e., that the dog-bone B specimen yields significantly higher fatigue lives when compared to the fatigue lives measured with the rectangular specimen. For instance, the stress level corresponding to a fatigue life of 10^4 cycles was 604 MPa for the rectangular specimen and 656 MPa for the dog-bone B specimen.

The results suggest that the dog-bone B specimen is applicable for fatigue testing and provides more reliable fatigue lives for UD and quasi-UD laminates when compared to the reference specimens. In addition, the dog-bone specimen enables the monitoring of damage accumulation in the gauge section to the number of cycles that result in the laminate fatigue failure.
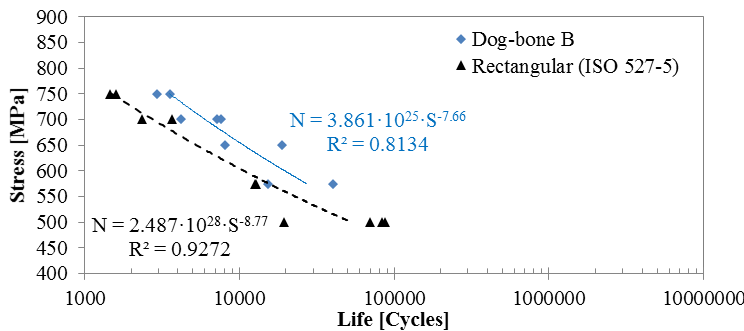
Figure 18. *S-N* curves for the quasi-UD stitched fabric reinforced laminate measured with the rectangular and dog-bone B test specimens.

The fatigue test data and the corresponding *S-N* curves measured using the dog-bone B specimen for the UD powder-bound and quasi-UD stitched fabric reinforced laminates reveal a slightly lower slope of the *S-N* curve and over ten-fold fatigue life for the UD powder-bound fabric reinforced laminate (see Figure 19). Mandell and Samborsky (1997) have observed a similar tendency, as they report that removing the stitching from quasi-UD NCFs before infusion improved fatigue life and lowered the slope of the fitted *S-N* curve. Samborsky et al. (2012) studied the influence of the presence of backing bundles in quasi-UD

NCFs. They observed that fatigue lives improved significantly for polyester laminates, but only slightly for epoxy laminates without backing bundles. The small difference measured for epoxy-based laminates may result from the rectangular specimen that they used in their tests. The main reason for the better fatigue performance measured in this study for the UD powder-bound fabric reinforced laminate is most probably the improved fibre straightness resulting from the absence of backing bundles and stitching. For instance, Mattson et al. (2007) have reported that the stitching and backing bundles in NCFs cause fibre undulation, which lowers fatigue performance. The other reasonmay be a stress concentration effect resulting from the transverse cracks in the backing bundles of the quasi-UD laminates. Zangeberg et al. (2014b) have suggested that an initial failure of the backing bundles (cracks) of quasi-UD GFRP laminates forms a stress concentration and a fretting/rubbing mechanism that gives rise to broken fibres in the axial bundles.

Based on the results, the UD laminate yielded considerably higher fatigue lives and a slightly lower *S-N* curve slope, meaning that the UD laminate makes it possible to manufacture lighter structures.
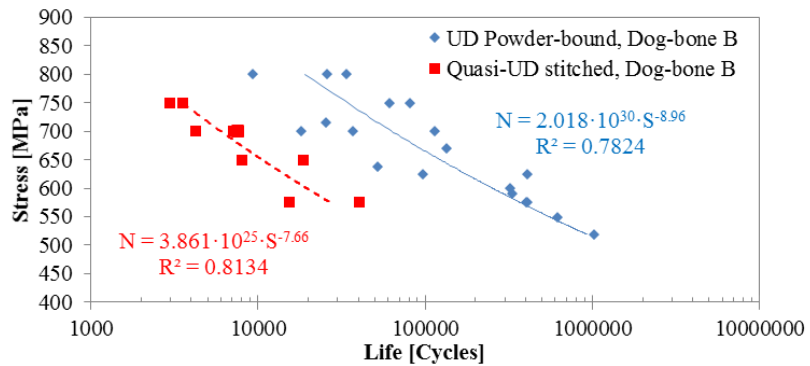
Figure 19. Comparison of the fatigue data for UD powder-bound fabric and quasi-UD stitched fabric -reinforced laminates.

4.2 The effect of stitch pattern and stitch tension on internal structure and fatigue properties of quasi-UD NCF laminates (P2)

The research continued with a study on how the controllable stitching parameters, i.e. the stitch pattern and stitch tension, contribute to the fibre volume fraction, axial fibre waviness, fatigue damage evolution and fatigue performance of quasi-UD laminates (Publication 2).

4.2.1 Measured fibre volume fractions

The fibre volume fraction (FVF) was determined using the resin burn-off technique to see possible differences in FVFs between the test laminates with different stitch patterns and tensions. The FVF was measured only with two samples

for each series. Therefore, the average values were only calculated since stand-ard deviations are meaningless to present. The results showed that the tricot stitch pattern resulted in a clearly higher FVF than the other stitch patterns, which provided almost equal FVFs (Table 2). This is explained by the less constraining tricot stitching that resulted in wider and more compressible (lower) bundles and thus a thinner laminate. The FVFs of the laminates with high and low tension double tricot stitch patterns were almost the same. Because the FVF affects the fatigue performance in general, the FVF difference must be noted when fatigue test results between these types of laminates are compared.

Table 2. Measured average fibre volume fractions of quasi-UD laminates with different stitch patterns and tensions.

Stitch pattern	Stitch tension	Fibre volume fraction [%]
Tricot	High	57.5
Tricot-straight double	High	54.4
Double tricot	High	54.1
Double tricot	Low	53.5

4.2.2 Internal structure and axial fibre waviness

The cross-sectional micrographs indicated that the average width and height of the axial load carrying fibre bundles and the average resin channel width between the adjacent axial bundles considerably differed in the laminates with different stitch patterns (see Figure 20 (Ia,IIa,IIIa)). The results also revealed that the effect of stitch tension on the above parameters was minor in between the stitch loops but statistically significant at the stitch loop cross-sections (see Figure 20 (Ib,IIb,IIIb)). Therefore, it is clear that the higher stitch tension compresses more the fibre bundles at the points of the stitch loops since the average width of the bundles (Figure 20 (Ib)) was lowest and the resin channel widest (Figure 20 (IIIb)) at the points of the stitch loops along the stitch length. The results also revealed that the average height of the bundles was lowest between the double tricot stitch loops at the point where the stitch threads cross each other (Figure 20 (IIb)).
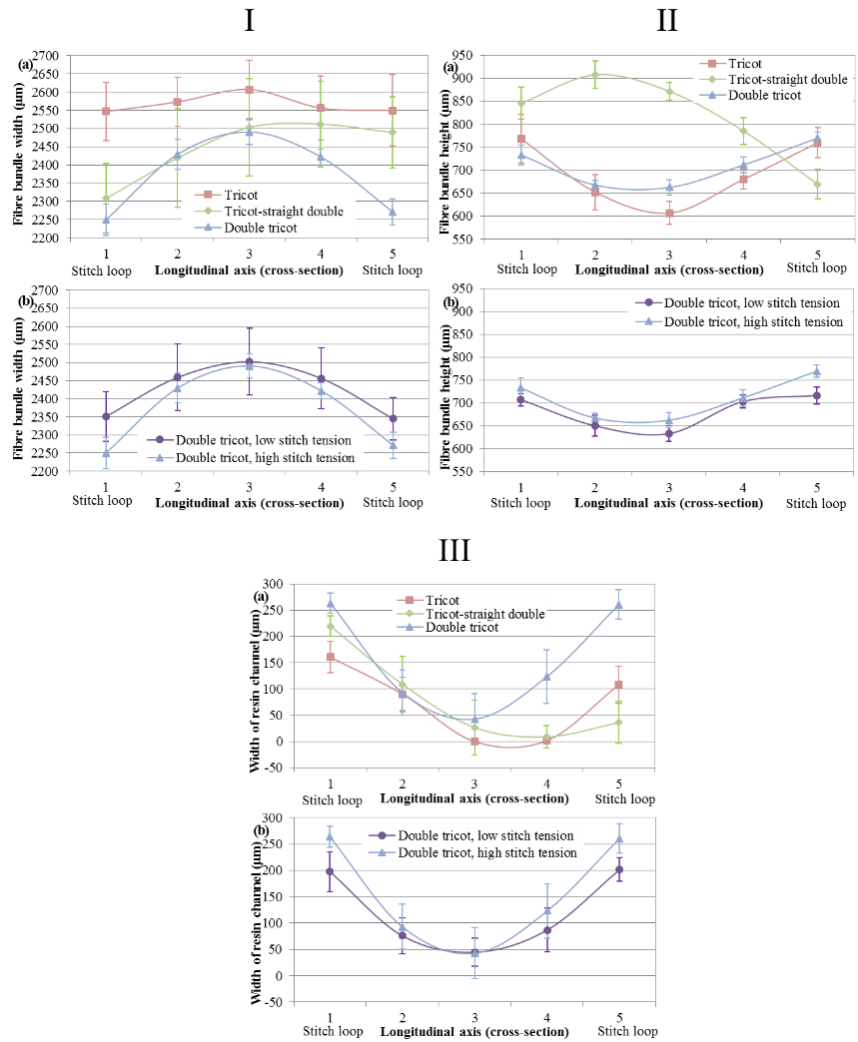
Figure 20. Average (I) width and (II) height of the axial fibre bundles and (III) resin channel width within the stitch length in test laminates. Subfigures (a) represent laminates with high tension tricot, tricot-straight double and double tricot stitch patterns, and subfigures (b) laminates with low and high tension double tricot stitch patterns.

The cross-sectionals also revealed that the mutual location of axial fibre bundles and stitching in upper and lower fabrics varied in the test laminates. Axial fibre bundles in upper and lower fabrics were closely overlapping in the laminates with tricot and tricot-straight double stitches, whereas they located (closely) on top of each other in the laminates with double tricot stitches. The images taken perpendicular to the laminate plane (see Figure 22) showed that the stitching thread travelled in a reversed phase in upper and lower fabrics in the laminates with tricot, tricot-straight double and high-tension double tricot stitches. The stitches were in the same phase, that is, in the same location in the longitudinal direction, in the laminate with the low-tension double tricot stitch.

The results (Table 3) indicate that the stitch pattern affects both the in-plane waviness and out-of-plane misalignment angles of axial fibres. The tricot stitch pattern is sensitive to producing in-plane axial fibre bundle undulation, as the stitching thread zigzags around the bundle, moving the bundle laterally. The double tricot and tricot-straight double patterns periodically compress single bundles at the stitch loops, providing better fibre bundle straightness than the tricot stitch pattern. However, even with these stitch types, individual fibres undulate in between the stitch loops, as shown in Figure 20 (Ia,Ib).

A relatively high out-of-plane misalignment angle was measured for the tricot-straight double stitch pattern. Out-of-plane waviness of axial fibres is attributed to transversal fibre bundles and stitching, but the taken cross-sectionals (Figure 21) indicate that it is also attributed to the mutual location of adjacent fabrics. In case the axial fibre bundles do not lie on top of each other, they may partly be pressed between the bundles of the neighbouring fabric if the stitch thread (pattern) is not able to keep the fibres properly together. The results also suggest that stitch tension of the double tricot stitched reinforcement does not notably affect the in-plane waviness and out-of-plane fibre misalignment angle.

Table 3. Maximum out-of-plane misalignment angles of axial fibres and in-plane waviness of axial fibre bundles in the quasi-UD laminates with different stitch patterns and tensions (average ± standard deviation).

Stitch pattern	Stitch tension	Out-of-plane misalignment angle [°]	In-plane misalignment angle [°]
Tricot	High	4.5°	5.38° ± 0.78°
Tricot-straight double	High	6.8°	1.06° ± 0.62°
Double tricot	High	4.2°	0.67° ± 0.47 °
Double tricot	Low	4.3°	0.56° ± 0.60°
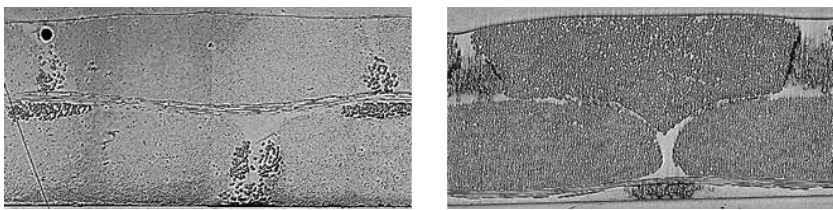
Figure 21. Cross-sections of the laminate with the tricot-straight double stitch pattern at the point of a stitch loop (left) and between stitch loops (right).

4.2.3 Fatigue damage evolution

The images taken during fatigue tests indicate that damage evolution depends on the stitch pattern but not on the stitch tension (Figure 22). Transverse cracks initiated in all laminates at the areas of the backing bundles already during the first load cycle. Earlier, Zangenberg et al. and Jespersen et al. (2015; 2016;

2014b) have also observed that transverse backing bundles act as damage initiators in quasi-UD NCF laminates during tensile fatigue testing.
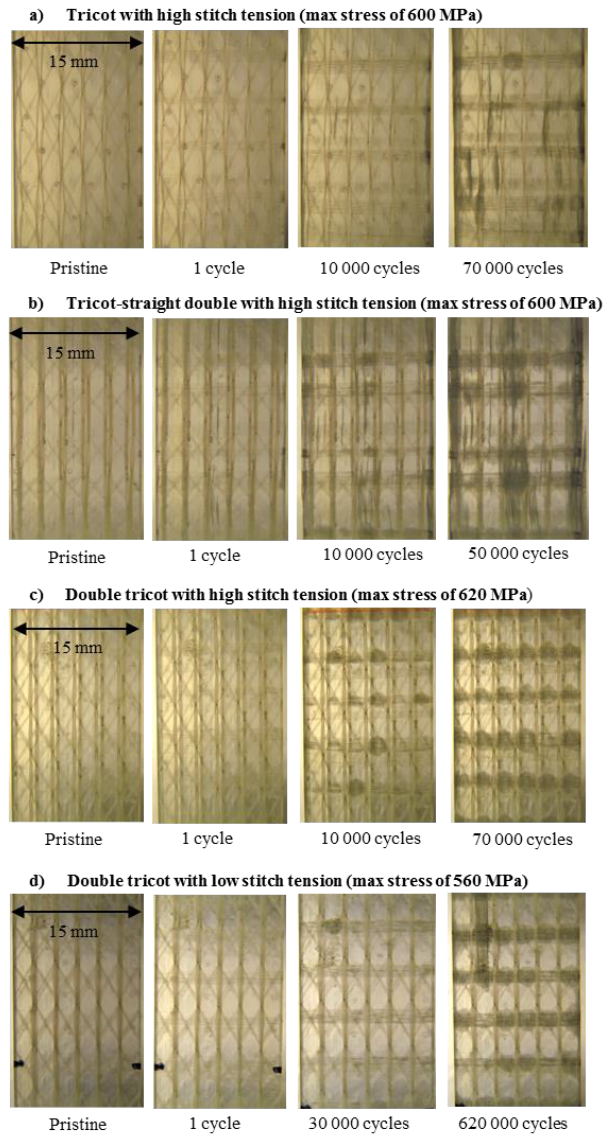
Figure 22. Damage evolution during fatigue tests of laminates with different stitch patterns and stitch tensions; the laminates subjected to maximum stress close to 600 MPa.

During a fatigue test, the quantity and length of axial cracks and their development rate varied in the laminates with different stitch patterns (Figure 22). The axial cracks initiated at the intersection areas of transverse bundles and propagated in between them in laminates with the tricot and tricot-straight double stitch patterns. In the laminates with the double tricot stitch pattern, axial cracks and local delaminations primarily concentrated at the intersection areas of transverse and axial bundles (see magnifications of damage types in Figure

23). The differences in damage evolution obviously result from differences in the waviness of axial fibres since wavy fibres tend to straighten in tensile loading resulting in fibre-matrix debonding and matrix damage (Piggott, 2002). Finally, specimens with the tricot stitch pattern failed in the gauge section but part of the specimens with the tricot-straight double and double tricot stitch patterns failed at the end tabs.
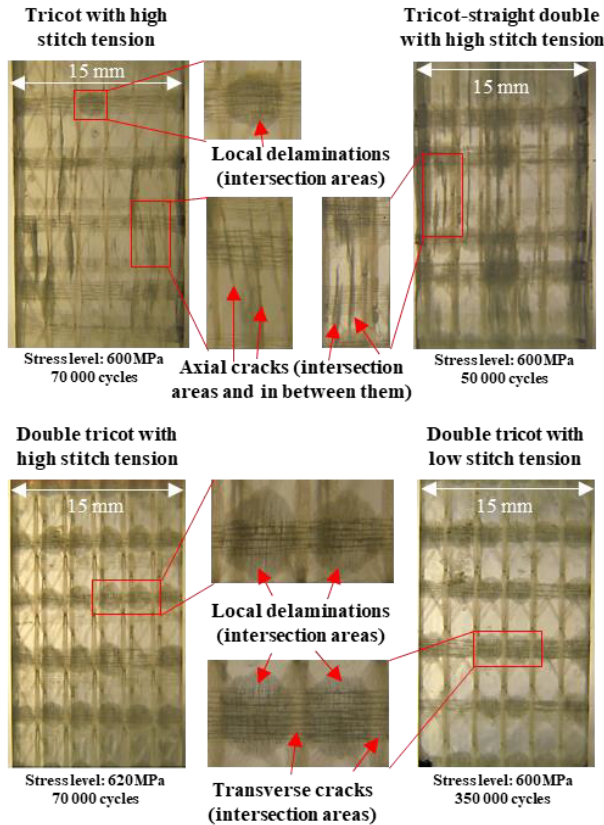
Figure 23. Typical damage types in the laminates with different stitch patterns and stitch tensions.

In the experimental work performed recently (Korkiakoski et al., 2016) for a quasi-UD NCF reinforced laminate with the tricot stitch pattern and stacking sequence of $[0°]_3$, all fatigue test specimens also failed in the gauge section as for the laminate with the tricot stitch pattern and a stacking sequence of $[0°]_2$ above. The authors suggested that some of the axial cracks and local delaminations occurred only in a certain fabric in the thickness direction of the laminate. However, they were not able to determine the exact location of the damage initiation in the thickness direction. The authors also reported that the fabrics were stacked rather randomly with respect to each other, that is, the mutual location of each fabric with respect to the neighbouring fabric varied so that axial and transverse fibre bundles and stitch loops located rather randomly with respect to each other.

The observed differences in the mutual location of axial bundles and stitching among the test laminates in this study and in the current literature (Korkiakoski et al., 2016) encourage studying systematically the effect of exact positioning of adjacent fabrics on the fatigue performance and damage development.

4.2.4 Fatigue performance

Fatigue test results (Figure 24) indicate a very small scatter ($R^2 > 0.94$) for all test series, meaning that the power regression commonly used to form an *S-N* curve accurately fitted the fatigue data. The specimens that failed at the tabbed area were also included when determining *S-N* curves since before final failure these specimens experienced high extent of axial cracks and/or local delaminations and several axial fibre breakages in the gauge section. In these specimens, the damages in the tabbed area were more detrimental and resulted in the specimens failing in the tabbed area. The measured fatigue lives of these specimens were also close to the fatigue lives of the specimens that failed in the gauge section. Furthermore, the coefficient of determination values, *R^2*, were very close to the value of 1.
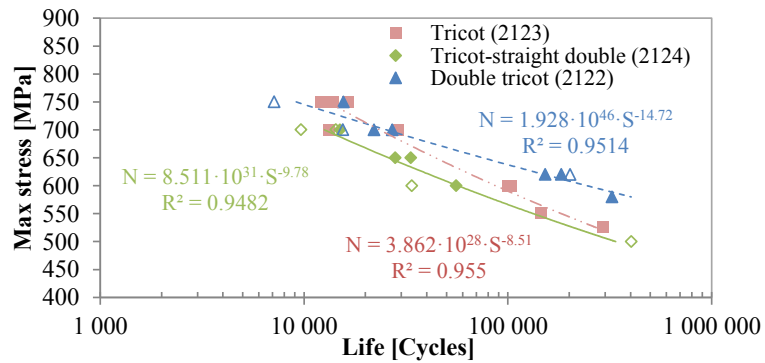
Figure 24. Fatigue test data and derived *S-N* curves for test laminates with different high tension stitch patterns. Filled markers represent specimens that failed in the gauge section and unfilled markers indicate specimens that failed at the tabbed area.

The fatigue test results show that the stitch pattern significantly affects the fatigue life and clearly affects the slope parameter of the *S-N* curve. The highest fatigue lives were measured for the laminates with double tricot stitched reinforcements, and the lowest for the laminate with tricot-straight double stitched reinforcement. When the specimens were subjected to 600 MPa maximum stress, the laminate with the double-tricot stitch pattern yielded close to three-fold and over four-fold fatigue lives when compared to the fatigue lives measured for the laminates with the tricot and tricot-straight double-stitch patterns, respectively. Vallons et al. (2014) have reported only small differences in fatigue lives between two quasi-UD GFRP laminates, which could result from the fact that the stitch patterns they used were close to each other and that they used rectangular specimens.

The fatigue tests conducted by Dharan (1975a) and Mandel and Samborsky (1997) for quasi-UD and "pure" UD GFRP laminates with different FVFs suggest that the slope of the *S-N* curve (*m* value) will steepen with an increasing FVF, indicating faster material degradation in cyclic loading. In addition, a high FVF results in high static strength of the laminate, implying that the *S-N* curve of the laminate will also shift towards higher stresses (Vallons et al., 2013). Thus, the measured *S-N* curves of the laminates with tricot and tricot-straight double stitch patterns might be close to each other if their FVF values were the same.

The fatigue performance difference between the laminates with different stitch patterns is assumed to depend mostly on the fibre waviness. Structural analyses and measured fatigue lives of the test laminates support this assumption. The in-plane waviness was lowest in the best performing laminate with the double tricot stitch pattern and highest in the laminate with the tricot stitch pattern. Additionally, the out-of-plane waviness of fibres in the weakest laminate with the tricot-straight double stitch pattern was clearly higher than in other laminates.

Fatigue performances of the laminates with high and low tension double tricot stitch patterns were also studied by comparing *S-N* curves calculated from the test data (Figure 25). The results indicate that the applied stitch tension has an insignificant effect on the fatigue life of the specimens. The in-plane and out-of-plane waviness of the axial fibres, as well as the fatigue damage evolution, were similar in both laminates with good accuracy, which explains the similarity of the fatigue test results.

Finally, it is noted that a higher number of specimens in each test series would have increased confidence with the test results (S-N curves), but a more extensive test program was not possible in the time frame of the study
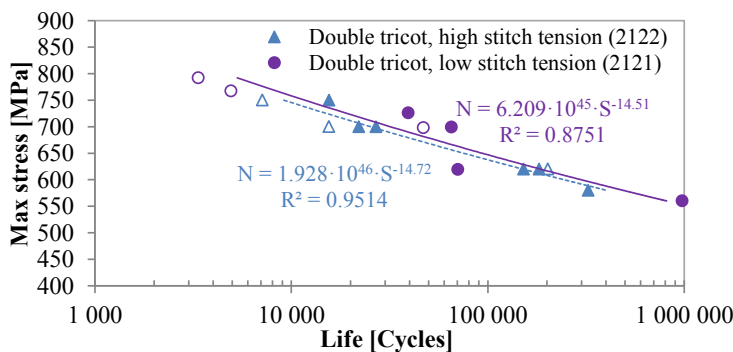

Figure 25. Fatigue test data and derived *S-N* curves for test laminates with high and low tension double tricot stitch patterns. Filled markers represent specimens that failed in the gauge section and unfilled markers indicate specimens that failed at the tabbed area.

4.3 The effect of fabric shifting on internal structure and fatigue properties of quasi-UD NCF laminates (P3)

Publication 2 of this thesis work and another recent study (Korkiakoski et al., 2016) indicated that the internal structure of a quasi-UD stitched fabric reinforced laminate clearly depends on the mutual location of adjacent fabrics. Therefore, research for the thesis was continued by studying in detail how the (practically) non-controllable stacking parameters, i.e., fabric shifting perpendicular and parallel to the axial fibre bundles, contribute to the fibre volume fraction, internal structure variation and axial fibre waviness. Fatigue tests were included in the study to find out how fabric shifting affects damage development and fatigue performance of quasi-UD laminates. Fabrics with a high-tension tricot stitch pattern were used as a reinforcement in all test laminates. The studied fabric shifting (lay-up) cases are listed in Table 4.

Table 4. Lay-up cases used in this study.

Lay-up	Mutual location of axial bundles	Mutual location of stitching
Case 1	On top of each other	Identical stitch phase
Case 2	Overlapping	Identical stitch phase
Case 3	On top of each other	Reversed stitch phase
Case 4	Overlapping	Reversed stitch phase

4.3.1 Measured fibre volume fractions

The fibre volume fraction (FVF) was determined using the resin burn-off technique for all test laminates. The results showed that the FVF was almost equal in the laminates (Table 5). Based on the results, it is clear that at least the fibre volume fraction does not affect the prospective difference in the fatigue performance between the laminates.

Table 5. Measured average fibre volume fraction of quasi-UD laminates with different fabric shifting cases.

Stitch pattern	Stitch tension	Lay-up	Fibre volume fraction [%]
Tricot	High	Case 1	58.0
Tricot	High	Case 2	57.7
Tricot	High	Case 3	58.0
Tricot	High	Case 4	58.5

4.3.2   Internal structure and axial fibre waviness

The results based on cross-sectional images showed that the average bundle width and height and the resin channel width varied along the stitch length in each laminate, as shown in Figure 26. The average bundle width (Figure 26a) was highest in between the stitch loops, and the average height (Figure 26b) and resin channel width (Figure 26c) were clearly highest at the stitch loops (cross sections 1 and 5) in each laminate. The results also suggest that the average width and height of the bundles and the average resin channel width are slightly affected by the fabric shift.
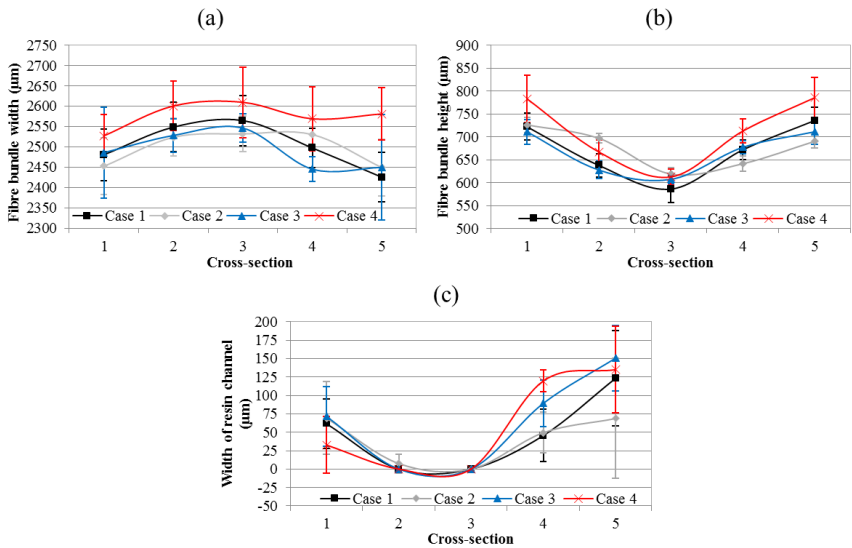

Figure 26. Average (a) width and (b) height of axial fibre bundles and (c) resin channel width in the laminates with different fabric shifting cases.

The in-plane waviness and out-of-plane misalignment angles of the axial fibres were determined for each test laminate, as described in Section 3.5. The results (see Table 6) suggest that fabric shifting slightly affects the in-plane waviness and out-of-plane misalignment angles. The out-of-plane misalignment angle was higher when the axial fibre bundles overlapped (Case 1 vs. Case 2, and Case 3 vs. Case 4). The lowest out-of-plane misalignment angle was in the laminate with the lay-up case 3, where the axial fibre bundles were on top of each other and the stitch phase was reversed between the fabrics. The highest out-of-plane misalignment angle was in the laminate with the lay-up case 4, where the fibre bundles were overlapping and the stitch phase was reversed between the fabrics. The relatively high out-of-plane misalignment with the lay-up case 4 might result from the fact that some of the bundles were pressed between adjacent bundles as observed for the laminate with the tricot-straight double stitch pattern in Section 4.2.2 (where the axial fibre bundles were also overlapping). The in-plane waviness of fibre bundles was slightly lower in the lay-up cases 3 and 4 (reversed stitch phase) compared to cases 1 and 2 (identical stitch phase) (see Table 6).

Table 6. Out-of-plane and in-plane misalignment angles in the quasi-UD laminates with different fabric positioning (average ± standard deviation).

Lay-up case	Out-of-plane misalignment angle [°]	In-plane misalignment angle [°]
Case 1	4.3°	5.0° ± 0.4°
Case 2	4.6°	5.4° ± 0.8°
Case 3	3.9°	4.6° ± 1.1 °
Case 4	6.6°	4.5° ± 0.3°

4.3.3 Fatigue damage evolution

Fatigue tests of this study phase were performed using only the developed dog-bone B specimen. The digital images taken during the fatigue tests suggest that fabric shifting affected damage evolution (Figure 27a-d). Transverse cracks initiated in all test specimens at the areas of backing fibre bundles already during the first load cycle. In the laminates with lay-up cases 1 and 2, where the stitch phase was identical between the fabrics, some axial cracks also developed during the first cycle. Later, new axial cracks developed and several fibres failed at the laminate surfaces in all laminates.

The size and location of axial cracks and local delaminations and their development rate were different in the test laminates. In the laminates with the lay-up cases 1 and 2, axial cracks initiated and propagated at the intersection areas of transverse and axial fibre bundles and in between the transverse bundles (Figure 27a and b). In the laminates with the lay-up cases 3 and 4, where the stitch phase was reversed between the fabrics, axial cracks or local delaminations primarily concentrated at the intersection areas (Figure 27c,d). Moreover, in the laminate with the lay-up case 4, axial cracks developed at a section where the stitch length in the upper fabric was locally slightly longer – obviously because of a stoppage of the warp-knitting machine during the NCF manufacturing process (Figure 27d).The region of the longer stitch phase in the entire width of the laminate (Case 4) was clearly the weakest in terms of fatigue, probably due to higher local fibre waviness.

The difference in the damage evolution between cases 1 and 3 partly results from the different degree of waviness of axial fibres. In addition, the axial fibre bundles in upper and lower fabrics with the lay-up cases 1 and 3 undulated in different phases. The bundles undulated in the same phase with Case 1 and in the opposite phase with Case 3. These differences apparently resulted in lower internal stress concentrations in the laminate, with the lay-up case 3 resulting in a slower damage evolution. In the laminates with the lay-up cases 1 and 2, the fabric shift perpendicular to the axial fibre bundles did not substantially affect the in-plane and out-of-plane fibre waviness and damage evolution. The laminates also had almost identical fatigue performances (see Section 4.3.4).
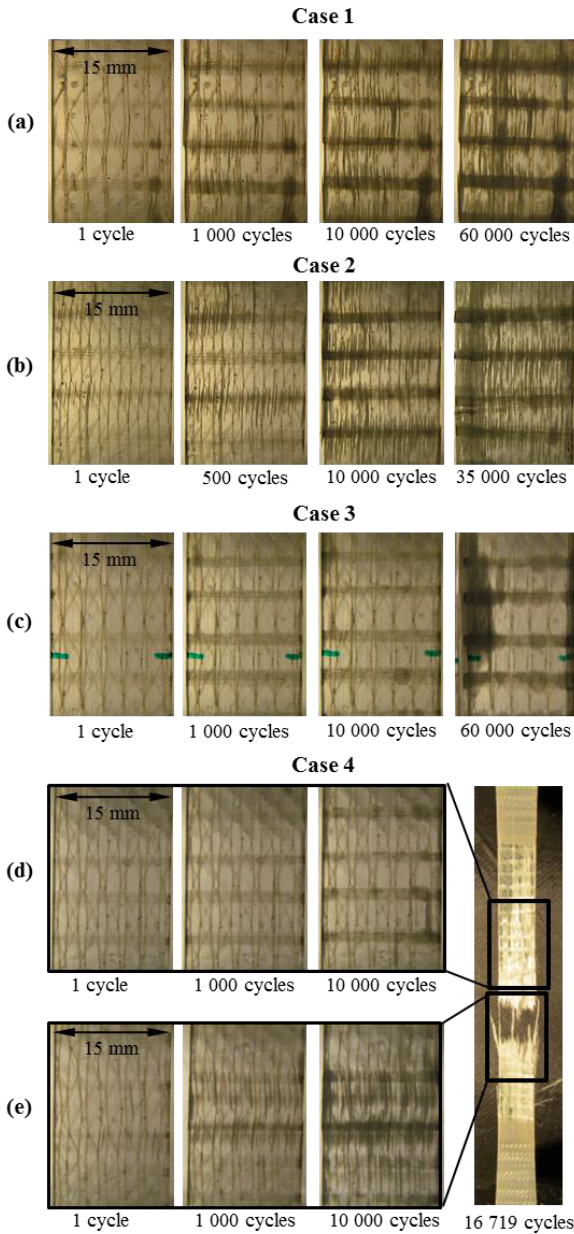
Figure 27. Damage progression during the fatigue tests in the laminates with different fabric shifting cases when subjected to a maximum stress of approximately 600 MPa.

4.3.4   Fatigue performance

Fatigue performance was studied by calculating *S-N* curves from the test data for all lay-up cases. The results (Figure 28) indicate a very small scatter (R^2 >0.93) for each laminate, meaning that the power regression accurately fitted the fatigue data. The results show that fabric shift significantly affected the fatigue life. The fatigue lives of laminates with the lay-up cases 1 and 2 were

almost identical, as were the measured fibre waviness values and damages in their fatigue tests. The laminate with the lay-up case 3 had a slower damage accumulation rate and significantly higher fatigue performance when compared to other laminates. The fatigue life of the laminate with the lay-up case 4 was clearly lowest due to premature failure of the specimens in the area of the stitch length change of the fabric in the gauge section. It should, however, be noted that all conclusions related to the fatigue performance of the laminate with the lay-up case 4 are very preliminary due to the fault of the fabric (due to the local stitch length change in the upper fabric).
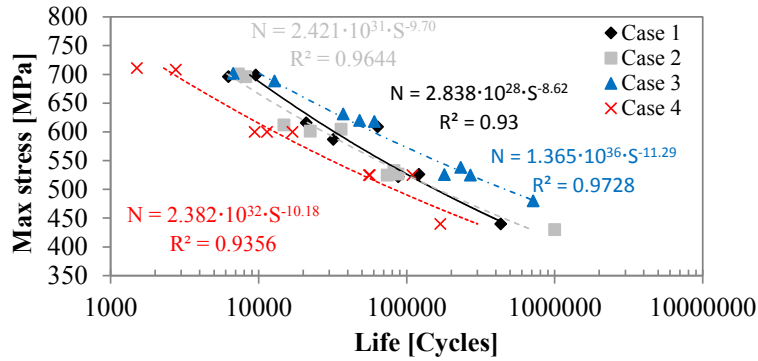

Figure 28. Fatigue test results and fitted *S-N* curves for test laminates with four different mutual locations of tricot-stitched fabrics.

The fatigue test results in Section 4.2.4 showed that the laminate with the tricot stitch pattern had a slope value of −8.51, which is close to the slope values calculated for the laminates with lay-up cases 1 and 2 (−8.62 and −9.70). The similarity in the slope values presumably results from the similar degree of waviness of axial fibres (See Table 3 and Table 6).

4.4 Compaction tests (P4)

Compaction tests of thick NCF preforms with the stacking sequence of $[0]_{10}$ were performed as part of the research (Publication 4). The aim was to measure how the stitch pattern and stitch tension as well as fabric shifting affect the thickness of the preform and fibre volume fraction of the laminate. The research also aimed to find out how well the fibre volume fractions measured for thin test laminates correspond with the fibre volume fractions of thicker laminates typically used in many composite structures.

4.4.1 Effect of stitch pattern on fibre compaction and fibre volume fraction

The effect of the stitch pattern on the dry compaction behaviour (how the preform thickness changes under vacuum pressure) was measured for preforms formed from fabrics with a high-tension tricot-straight double stitch pattern (2120), a low-tension double tricot stitch pattern (2121), and a high-tension tri-

cot stitch pattern (2123). The step compaction curves for the preforms presented in Figure 29 show a substantial effect of the stitch pattern on the final thickness of the preform at 0.9 bar vacuum pressure. The results also indicate that the preform formed from fabrics with the tricot stitch pattern (2123) is clearly thinner than the other preforms. One reason for the difference is apparently the higher amount of stitch thread in fabrics with double stitch patterns (2120 and 2121). The stitch pattern also affects the cross-sectional shape (thickness) of axial fibre bundles, and consequently the thickness of the preform. Vallons et al. (2014) studied compressibility of one layer of unimpregnated fabric between two circular stamps. They reported small thickness differences between two quasi-UD fabrics with almost the same stitch pattern.
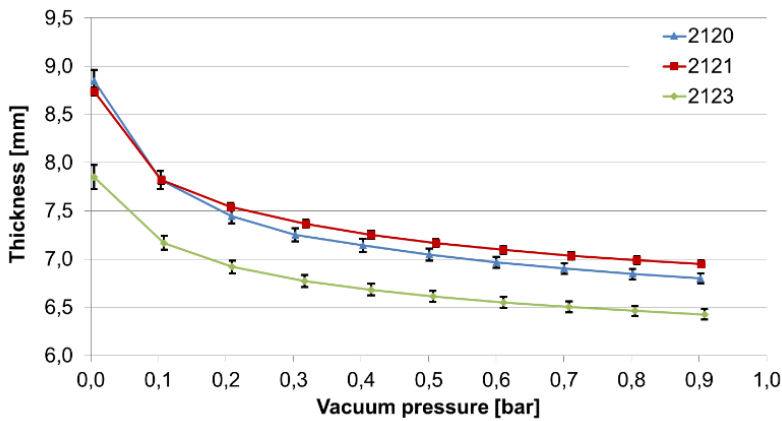

Figure 29. Step compaction curves with standard deviations for the preforms consisting of fabrics with a tricot stitch pattern (2123), a double tricot stitch pattern (2121) and a tricot-straight double stitch pattern (2120).

The effect of the stitch pattern and fibre type on the wet compaction behaviour was studied during the filling and post-filling stages of the preforms. The fibres of the fabrics (e.g. 2117 vs. 2121) were supplied by two different fibre manufacturers. Thus, it is expected that the fibres have a different type of sizing (coating). Measured thickness evolutions of the preforms are substantially different, as shown in Figure 30. The final thickness of the preform formed from the fabric with the tricot stitch pattern was clearly the lowest and the calculated final fibre volume fraction correspondingly the highest (Table 7). The preforms with the double tricot stitch had the highest final thicknesses. Different thickness values partly result from the amount of the stitch thread in the fabrics but also from different cross-sectional shapes of the axial fibre bundles. The calculated fibre volume fractions correspond quite well with the values measured for the test laminates formed from two fabrics (see Section 4.2.1). Vallons et al. (2014) reported small thickness differences between two quasi-UD laminates with almost the same stitch pattern. They explained that the difference results from the cross-sectional shape of the bundles. The difference might also result from the difference in the amount of stitch thread.
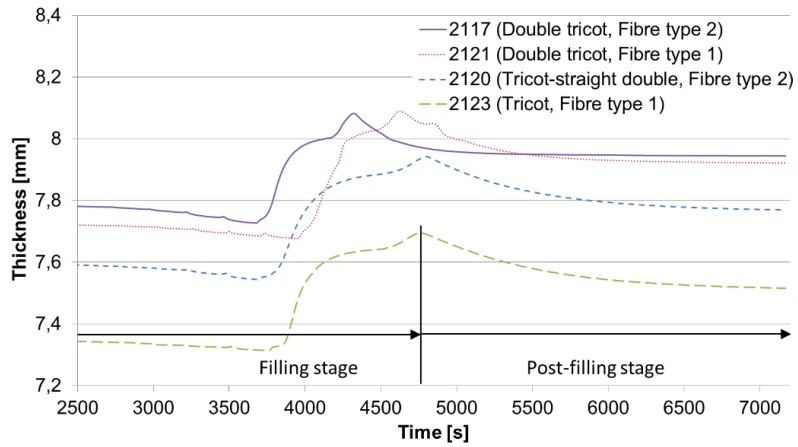
Figure 30. Thickness evolution of preforms with different stitch patterns during the filling and post-filling stages (wet compaction).

Table 7. Calculated fibre volume fractions for the laminates formed from fabrics with different stitch patterns.

Fabric	Fibre type	Stitch pattern	Final thickness (mm)	Final fibre volume fraction [%]
2117	2	Double tricot	7.944	56.45
2121	1	Double tricot	7.922	56.63
2120	2	Tricot-straight double	7.769	57.89
2123	1	Tricot	7.516	60.11

4.4.2 Effect of stitch tension and mutual location of axial fibre bundles on fibre compaction and fibre volume fraction

The effect of the stitch tension and the mutual location of axial fibre bundles (fibre bundles on top of each other or overlapping) on the dry compaction was studied during the pre-filling stage. The test materials were NCFs manufactured from two fibre types with low- and high-tension double stitch patterns.

Figure 31(a,b) presents measured step compaction curves for preforms manufactured from the Fibre Type 2 with low (2117) and high (2118) stitch tensions. Similarly, Figure 31(c,d) presents step compaction curves for the preforms manufactured from the Fibre Type 1 with low (2121) and high (2122) stitch tensions. The results suggest that the effect of the stitch tension on the final thickness of the preform is small. The final thickness of the preform was also close to the same with both fibre types.

The effect of the mutual location of axial fibre bundles in relation to each other (that is, fabric shift perpendicular to the axial fibre direction) can be studied by comparing the curves shown in each graph in Figure 31. It can be concluded that the overlapping lay-up compacts slightly more than the lay-up with fibre bun-

dles on top of each other. It should be noted that the lay-ups were slightly un-symmetrical, that is, the stabilizing 90° yarns were between the axial bundles in the preform. The unsymmetrical lay-up may have an effect on the compaction behaviour especially with the overlapping lay-up since the 90° yarns may decrease the nesting. It can be assumed that the overlapping lay-up would have been compacted even more if the adjacent two fabrics in the preform had been stacked so that the axial bundles had located side-by-side in the middle of the laminate.
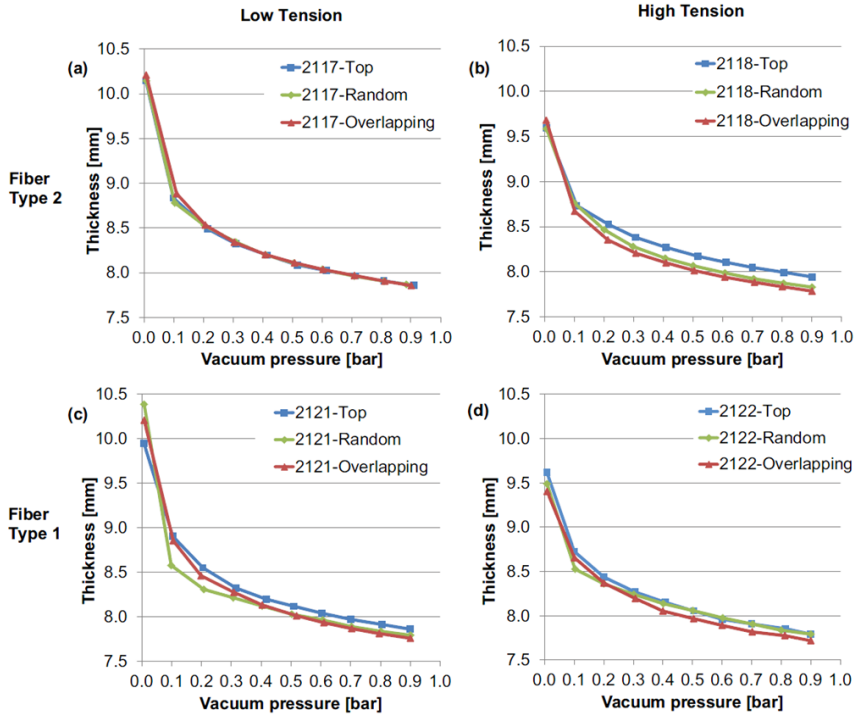
Figure 31. Step compaction curves for the preforms with a double tricot stitch pattern: (a) Fibre Type 2 and low stitch tension (2117), (b) Fibre Type 2 and high stitch tension (2118), (c) Fibre Type 1 and low stitch tension (2121), and (d) Fibre Type 1 and high stitch tension (2122).

The effect of the stitch tension on the wet compaction behaviour of the preforms during the filling and post-filling stages is shown in Figure 32a,b and in Figure 32c,d. The final thickness of the impregnated specimens with applied stitch tensions is seen to be nearly the same, i.e., the stitch tension did not have a considerable effect on the thickness and fibre volume fraction of the laminate (Table 8).

The effect of the mutual location of axial fibre bundles on the wet compaction can be studied by comparing the curves shown in each graph in Figure 32. The results indicate that the overlapping lay-up compacts slightly more than the lay-up with the fibre bundles on top of each other due to the better nesting ability

of bundles in the overlapping lay-up. The differences in laminate thickness values and in fibre volume fractions are anyhow relatively small (Table 8). The mutual location of the bundles does not only affect the thickness and FVF of the laminate. Fang et al. (2015) reported that the out-of-plane permeability of UD fabrics was two-fold larger with fibre bundles on top of each other (minimum nesting) than with fibre bundles overlapping (maximum nesting).

The FVFs reported in Publication 3 for thin fatigue test laminates with different lay-up cases were also close to each other (see Section 4.3.1). The values are mostly consistent with the values measured in compaction tests. An exception is the Case 2 test laminate (fibre bundles overlapping), for which a slightly lower FVF was measured when compared to the corresponding laminate with fibre bundles on top of each other. This inconsistency may result from that the FVF values in Publication 3 were determined only from two samples.
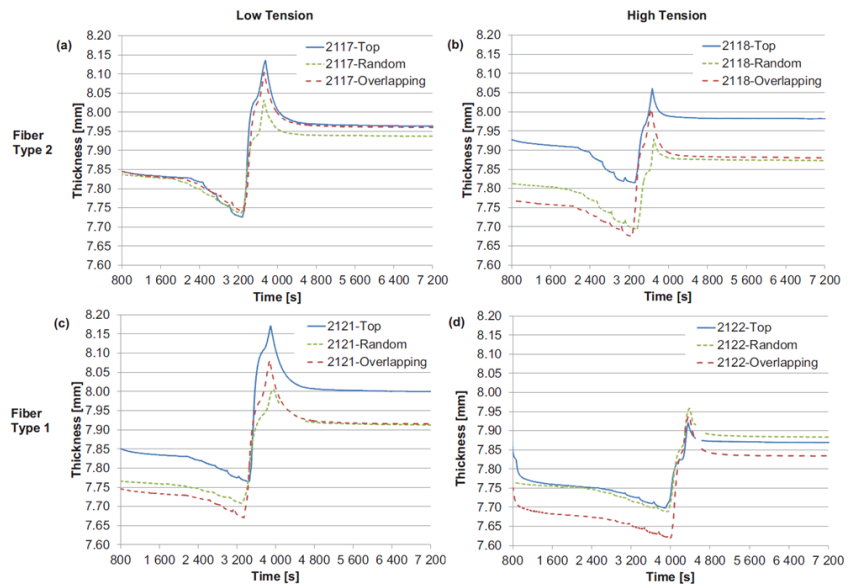
Figure 32. Effect of the mutual location of axial fibre bundles and stitch tension on preform thickness during the filling and post-filling stages: (a) low stitch tension and Fibre Type 2 (2117), (b) high stitch tension and Fibre Type 2 (2118), (c) low stitch tension and Fibre Type 1 (2121), and (d) high stitch tension and Fibre Type 1 (2122).

Table 8. Final thickness values and calculated fibre volume fractions for laminates with axial fibre bundles on top of each other or overlapping.

Fabric	Lay-up	Final thickness (mm)	Final fibre volume fraction [%]
2117	Top	7.964	56.29
	Overlapping	7.960	56.51
2118	Top	7.982	56.15
	Overlapping	7.880	57.00
2121	Top	8.000	56.01
	Overlapping	7.915	56.68
2122	Top	7.877	57.00
	Overlapping	7.834	57.34

5. Conclusions

5.1 Theoretical implications

The performed fatigue tests showed that the measured fatigue lives of the GFRP UD laminate were significantly dependent on the specimen geometry. The fatigue lives measured with the developed dog-bone B specimen were over nine-fold when compared to the fatigue lives measured with the rectangular test specimen and over three-fold when compared to the fatigue lives measured with the dog-bone A test specimen. All rectangular and dog-bone A specimens failed at the end tab area. However, several dog-bone B specimens experienced severe damages in the gauge section and often seemed to fail in the gauge section. Thus, the measured fatigue lives are at least much closer to the true fatigue lives of the laminate when compared to the values measured with other specimen types. Lower shear stresses in the dog-bone B specimen at least delayed the edge splitting. Different end tab material constituents, adhesives for the end tab bonding, and manufacturing procedures are other reasons that may have delayed damages in the tabbed area and resulted in higher fatigue lives when compared to fatigue lives measured with the dog-bone A specimen.

The thesis revealed that the in-plane and out-of-plane waviness of axial fibres considerably differ in quasi-UD laminates with different stitch patterns but not with the applied stitch tensions. Damage evolution in the laminates and consequently the measured fatigue lives (*S-N* curves) were significantly dependent on the stitch pattern, while they were not dependent on the stitch tension. For example, fabrics with the double-tricot stitch pattern yielded close to three-fold and over four-fold fatigue lives in the fatigue tests when compared to the fabrics with the tricot and tricot-straight double-stitch, respectively, when the specimens were subjected to 600 MPa maximum stress. Artefacts in the fabrics due to stitching, such as in-plane and out-of-plane waviness of axial fibres, were the most sensitive parameters affecting fatigue damage evolution. However, the mutual location of axial fibre bundles and stitch phase also varied between the laminates (fabric shifting).

Based on the test results, the mutual perpendicular location of tricot-stitched fabrics, that is, the shift of a fabric layer perpendicular to axial fibre bundles, does not significantly affect the damage development rate and fatigue life of a quasi-UD GFRP laminate. However, fabric shift parallel to the axial fibre bundles (i.e., the stitch phase difference between the fabrics) has a significant effect

on the damage development rate and fatigue life. The laminate with a reversed stitch phase between the neighbouring fabrics showed a considerably lower damage development rate and a significantly increased fatigue life when compared to the laminate with an identical stitch phase. The best performing laminate with the reversed stitch phase (lay-up case 3) yielded 83% higher fatigue life at a 600 MPa stress level and a 30% lower *S-N* curve slope than the laminate with the identical stitch phase (lay-up case 1). The waviness of the axial load-carrying fibre bundles and the difference in the phase of axial fibre bundle in-plane waviness between the fabrics were the most sensitive parameters affecting the fatigue performance.

Worth noting is that all test laminates were manufactured using the same resin/hardener system. Another system might result in different fatigue lives. However, since the differences measured in fatigue performances are due to geometric differences, the mutual order in fatigue performances of the laminates obviously remains the same if the resin system is changed. In addition, the effects of fabric shift were measured only for tricot-stitched fabric reinforced laminates, i.e., they may not be the same in laminates reinforced with other types of stitched fabrics. Nevertheless, it is obvious that differences in mutual locations of neighbouring fabrics also result in a scatter in the fatigue performance of quasi-UD laminates reinforced with other types of stitched fabrics.

The performed compaction study specifically revealed that the applied stitch tensions did not affect the compaction behaviour of dry and resin-impregnated preforms. However, the stitch pattern substantially affected the compaction behaviour of both dry and resin-impregnated preforms, resulting also in a variation in the fibre volume fraction. The dry preforms with the double tricot stitch pattern and the tricot-straight double stitch pattern had 8.1% and 5.8% higher thickness, respectively, than the preform with the tricot stitch pattern under 0.9 bar vacuum. The resin-impregnated preform with the double tricot stitch pattern had 5.4-5.7% and with the tricot-straight double stitch pattern 3.4% higher final thickness than the preform with the tricot stitch pattern. In addition, the fabric shift perpendicular to axial fibre bundles had a small but detectable effect on the compaction behaviour of UD NCF preforms. In the dry and wet compaction tests, preforms with overlapping fibre bundles compacted slightly more effectively than the preforms with fibre bundles lying on top of each other, bearing in mind that the total measurement error was ±0.05 mm. The results also showed that fibre volume fractions measured for thick preforms correspond well to the fibre volume fractions measured for thin test laminates.

5.2 Recommendations for future studies

The fatigue tests of UD laminates and quasi-UD laminates with double tricot stitch and tricot-straight double stitch patterns revealed that part of the type B dog-bone specimens still failed at the end tabs. Thus, there is a need to further improve the specimen to obtain fatigue lives that are true or closer to the true

life of the material systems being tested. It would also be beneficial to find out how the type B specimen and its possible derivatives perform in fatigue tests of UD-laminates reinforced with other types of fibres (e.g. natural and aramid fibres).

The study also revealed that a reduction in the maximum shear stress value at the edges of the specimen and in the area with high shear stress reduced specimen splitting and increased the measured fatigue lives. Since these values are affected by the in-plane curvature of the specimen, the in-plane shape should be developed further to improve the measured fatigue lives. In addition, the effect of the end tab material, adhesive and the bonding process should be studied in more detail since they may considerably affect stresses in the bond line and detachment features of the end tabs.

It was further found out that the applied stitch tension (low or high) of the double tricot stitch pattern did not affect damage evolution and fatigue performance of quasi-UD laminates. The in-plane and out-of-plane waviness of axial fibre bundles within the stitch length were also close to the same with both stitch tensions. However, it is notable that the effect of stitch tension was studied only with the double tricot stitch pattern. A natural extension of the study would be to measure the effects of stitch tension with other stitch patterns.

The effect of fabric shift on laminate fatigue performance was also studied only with tricot-stitched fabrics. Extending this study to reinforcements with other stitch patterns would provide a wider view on the scatter in the fatigue performance of quasi-UD laminates due to fabric shift.

References

Aono, Y., Hirota, K., Lee, S., Kuroiwa, T., & Takita, K. (2008). Fatigue damage of GFRP laminates consisting of stitched unit layers. *International Journal of Fatigue, 30*(10), 1720-1728.

Asp, L. E., Edgren, F., & Sjögren, A. (2004). Effects of stitch pattern on the mechanical properties of non-crimp fabric composites. *In: 11th European Conference on Composite Materials (ECCM11).* Rhodes, Greece.

ASTM E739-91. (2004). Standard practice for statistical analysis of linear or linearized stress-life (SN) and strain-life (eN) fatigue data. *ASTM International, West Conshohocken, PA.*

Aymerich, F., Priolo, P., Sanna, R., & Sun, C. (2001). Fatigue behaviour of stitched composite laminates. *Proceedings of the 13th International Conference on Composite Materials (ICCM13),* Beijing, China. 25-29.

Aymerich, F., Priolo, P., & Sun, C. (2003). Static and fatigue behaviour of stitched graphite/epoxy composite laminates. *Composites Science and Technology, 63*(6), 907-917.

Bibo, G., Hogg, P., & Kemp, M. (1997). Mechanical characterisation of glass-and carbon-fibre-reinforced composites made with non-crimp fabrics. *Composites Science and Technology, 57*(9), 1221-1241.

Brøndsted, P., Lilholt, H., & Lystrup, A. (2005). Composite materials for wind power turbine blades. *Annu.Rev.Mater.Res., 35*, 505-538.

Brouwer, W. D., Van Herpt, E. C. F. C., & Labordus, M. (2003). Vacuum injection moulding for large structural applications. *Composites Part A: Applied Science and Manufacturing, 34*(6 SPEC.), 551-558.

Carvelli, V., & Lomov, S. V. (2015). *Fatigue of textile composites,* Elsevier.

Carvelli, V., Tomaselli, V. N., Lomov, S. V., Verpoest, I., Witzel, V., & Broucke, B. V. d. (2010). Fatigue and post-fatigue tensile behaviour of non-crimp stitched and unstitched carbon/epoxy composites. Composite Science and Technology, 70, 2216-2224.

Curtis, P. (1988). *CRAG (composite research advisory group) test methods for the measurement of the engineering properties of fibre reinforced plastics. No. RAE TR-88012. ROYAL AEROSPACE ESTABLISHMENT, FARNBOROUGH, UNITED KINGDOM.*

Curtis, P. (1991). Tensile fatigue mechanisms in unidirectional polymer matrix composite materials. *International Journal of Fatigue, 13*(5), 377-382.

De Baere, I., Van Paepegem, W., & Degrieck, J. (2009). On the design of end tabs for quasi-static and fatigue testing of fibre-reinforced composites. *Polymer Composites, 30*(4), 381-390.

Dharan, C. (1975a). Fatigue failure in graphite fibre and glass fibre-polymer composites. *Journal of Materials Science, 10*(10), 1665-1670.

Dharan, C. (1975b). Fatigue failure mechanisms in a unidirectionally reinforced composite material. *Fatigue of composite materials*, ASTM International.

Drapier, S., & Wisnom, M. R. (1999). Finite-element investigation of the compressive strength of non-crimp-fabric-based composites. *Composites Science and Technology, 59*(8), 1287-1297.

Edgren, F., Mattsson, D., Asp, L. E., & Varna, J. (2004). Formation of damage and its effects on non-crimp fabric reinforced composites loaded in tension. *Composites Science and Technology, 64*(5), 675-692.

Fang, L., Jiang, J., Wang, J., & Deng, C. (2015). Effect of nesting on the out-of-plane permeability of unidirectional fabrics in resin transfer molding. *Applied Composite Materials, 22*(3), 231-249.

Fang, L., Jiang, J., Wang, J., Deng, C., Li, D., & Liu, F. (2014). Effect of layer shift on the out-of-plane permeability of 0°/90° noncrimp fabrics. *Journal of Reinforced Plastics and Composites, 33*(22), 2073-2094.

Gamstedt, E. K., Berglund, L. A., & Peijs, T. (1999). Fatigue mechanisms in unidirectional glass-fibre-reinforced polypropylene. *Composites Science and Technology, 59*(5), 759-768.

Govignon, Q., Bickerton, S., & Kelly, P. (2010). Simulation of the reinforcement compaction and resin flow during the complete resin infusion process. *Composites Part A: Applied Science and Manufacturing, 41*(1), 45-57.

Govignon, Q., Bickerton, S., & Kelly, P. (2013). Experimental investigation into the post-filling stage of the resin infusion process. *Journal of Composite Materials, 47*, 1479-1492.

Govignon, Q., Bickerton, S., Morris, J., & Kelly, P. (2008). Full field monitoring of the resin flow and laminate properties during the resin infusion process. *Composites Part A: Applied Science and Manufacturing, 39*(9), 1412-1426.

Hammami, A. (2001). Effect of reinforcement structure on compaction behavior in the vacuum infusion process. *Polymer Composites, 22*(3), 337-348.

Harris, B. (2003). *Fatigue in composites: Science and technology of the fatigue response of fibre-reinforced plastics,* Woodhead Publishing.

ISO 527-5 (2009) Plastics—determination of tensile properties—Part 5: Test conditions for unidirectional fibre-reinforced plastic composites. *European Committee for Standardization, Brussels, Belgium.*

Jespersen, K. M., Lowe, T., Withers, P. J., Zangenberg, J., & Mikkelsen, L. P. (2015). Micromechanical time-lapse X-ray CT study of fatigue damage in uni-directional fibre composites. *Proceedings of the 20th International Conference on Composite Materials (ICCM20), Copenhagen, Denmark.*

Jespersen, K. M., Zangenberg, J., Lowe, T., Withers, P. J., & Mikkelsen, L. P. (2016). Fatigue damage assessment of uni-directional non-crimp fabric reinforced polyester composite using X-ray computed tomography. *Composites Science and Technology, 136*, 94-103.

Kelly, P., Umer, R., & Bickerton, S. (2006). Viscoelastic response of dry and wet fibrous materials during infusion processes. *Composites Part A: Applied Science and Manufacturing, 37*(6), 868-873.

Kensche, C. (1996). *Fatigue of materials and components for wind turbine rotor blades, EUR 16684, European commission, Luxenbourg 1996.*

Kensche, C. W. (2006). Fatigue of composites for wind turbines. *International Journal of Fatigue, 28*(10), 1363-1374.

Korkiakoski, S., Kanerva, M., & Saarela, O. (2016). Fatigue testing of quasi-UD and cross-ply reinforced composites: The recent achievements of test specimen generation. *In: 17th European Conference on Composite Materials (ECCM17).* Munich, Germany.

Lekakou, C., Edwards, S., Bell, G., & Amico, S. (2006). Computer modelling for the prediction of the in-plane permeability of non-crimp stitch bonded fabrics. *Composites Part A: Applied Science and Manufacturing, 37*(6), 820-825.

Lomov, S. (2011). In Lomov S. (Ed.), *Non-crimp fabric composites: Manufacturing, properties and applications,* Woodhead publishing.

Lomov, S. V., Verpoest, I., Peeters, T., Roose, D., & Zako, M. (2003). Nesting in textile laminates: Geometrical modelling of the laminate. *Composites Science and Technology, 63*(7), 993-1007.

Lundström, T. S. (2000). The permeability of non-crimp stitched fabrics. *Composites Part A: Applied Science and Manufacturing, 31*(12), 1345-1353.

Luo, Y., & Verpoest, I. (1999). Compressibility and relaxation of a new sandwich textile preform for liquid composite molding. *Polymer Composites, 20*(2), 179-191.

Mandell, J. F., Reed, R. M., & Samborsky, D. D. (1992). *Fatigue of fiberglass wind turbine blade materials, Sandia national laboratories.*

Mandell, J. F., Reed, R. M., Samborsky, D. D., & Pan, Q. (1993). Fatigue performance of wind turbine blade composite materials. *Wind Energy, 14*, 191-198.

Mandell, J. F., & Samborsky, D. D. (1997). *DOE/MSU composite material fatigue database: Test methods, materials, and analysis.* Sandia National Laboratories, Albuquerque, NM (United States).

Mattsson, D., Joffe, R., & Varna, J. (2007). Methodology for characterization of internal structure parameters governing performance in NCF composites. *Composites Part B: Engineering, 38*(1), 44-57.

Miller, A. (1996). *The effect of microstructural parameters on the mechanical properties of non-crimp fabriccomposites* (PhD thesis), Cranfield University, United Kindom.

Minitab 17, for windows, 2014

Mouritz, A. (2004). Fracture and tensile fatigue properties of stitched fibreglass composites. *Proceedings of the Institution of Mechanical Engineers, Part L: Journal of Materials Design and Applications, 218*(2), 87-93.

Nijssen, R. P. L. (2006). Fatigue life prediction and strength degradation of wind turbine rotor blade composites. *(PhD thesis) Delft University of Technology, Netherlands.*

Nijssen, R. P. L. (2014). *"OptiDat database", knowledge centre WMC, http://Www.wmc.eu/optimatblades_optidat.php, (accessed juli 28, 2014).*

Nordlund, M., & Lundstrom, T. S. (2005). Numerical study of the local permeability of noncrimp fabrics. *Journal of Composite Materials, 39*(10), 929-947.

Nordlund, M., Lundström, T. S., Frishfelds, V., & Jakovics, A. (2006). Permeability network model for non-crimp fabrics. *Composites Part A: Applied Science and Manufacturing, 37*(6), 826-835.

Piggott, M. R. (2002). *Load bearing fibre composites.* Springer Science & Business Media.

Qian, C. (2013). Multi-scale modelling of fatigue of wind turbine rotor blade composites. *(PhD thesis), Delf University of Technology, Netherlands.*

Samborsky, D., Mandell, J., & Miller, D. (2012). The SNL/MSU/DOE fatigue of composite materials database: Recent trends. *53rd AIAA/ASME/ASCE/AHS/ASC Structures, Structural Dynamics and Materials Conference 20th AIAA/ASME/AHS Adaptive Structures Conference 14th AIAA,* Honolulu, Hawaii.

Summerscales, J., & Searle, T. (2005). Low-pressure (vacuum infusion) techniques for moulding large composite structures. *Proceedings of the Institution of Mechanical Engineers, Part L: Journal of Materials Design and Applications, 219*(1), 45-58.

Tackitt, K. D., & Walsh, S. M. (2005). Experimental study of thickness gradient formation in the vartm process. *Materials and Manufacturing Processes, 20*(4), 607-627.

Tessitore, N., & Riccio, A. (2006). A novel FEM model for biaxial non-crimp fabric composite materials under tension. *Computers & Structures, 84*(19–20), 1200-1207.

Toll, S. (1998). Packing mechanics of fiber reinforcements. *Polymer Engineering & Science, 38*(8), 1337-1350.

Toll, S., & Manson, J. (1995). Elastic compression of a fiber network. *Journal of Applied Mechanics, 62*(1), 223-226.

Truong, T. C., Vettori, M., Lomov, S., & Verpoest, I. (2005). Carbon composites based on multi-axial multi-ply stitched preforms. part 4. mechanical properties of composites and damage observation. *Composites Part A: Applied Science and Manufacturing, 36*(9), 1207-1221.

Vallons, K. (2009). The behaviour of carbon fibre-epoxy NCF composites under various mechanical loading conditions. (PhD thesis), Katholieke Universiteit Leuven, Belgium.

Vallons, K., Adolphs, G., Lucas, P., Lomov, S. V., & Verpoest, I. (2013). Quasi-UD glass fibre NCF composites for wind energy applications: A review of requirements and existing fatigue data for blade materials. *Mechanics & Industry, 14*(03), 175-189.

Vallons, K., Adolphs, G., Lucas, P., Lomov, S. V., & Verpoest, I. (2014). The influence of the stitching pattern on the internal geometry, quasi-static and fatigue mechanical properties of glass fibre non-crimp fabric composites. *Composites Part A: Applied Science and Manufacturing, 56*, 272-279.

Vassilopoulos, A. P., & Keller, T. (2011). *Fatigue of fiber-reinforced composites* Springer Science & Business Media.

Verpoest, I., & Lomov, S. V. (2005). Virtual textile composites software WiseTex: Integration with micro-mechanical, permeability and structural analysis. *Composites Science and Technology, 65*(15), 2563-2574.

Williams, C., Grove, S., & Summerscales, J. (1998). The compression response of fibre-reinforced plastic plates during manufacture by the resin infusion under flexible tooling method. *Composites Part A: Applied Science and Manufacturing, 29*(1), 111-114.

Yang, J., Xiao, J., Zeng, J., Jiang, D., & Peng, C. (2012). Compaction behavior and part thickness variation in vacuum infusion molding process. *Applied Composite Materials, 19*(3-4), 443-458.

Yenilmez, B., & Sozer, E. M. (2009). Compaction of e-glass fabric preforms in the vacuum infusion process, A: Characterization experiments. *Composites Part A: Applied Science and Manufacturing, 40*(4), 499-510.

Yuexin, D., Zhaoyuan, T., Yan, Z., & Jing, S. (2008). Compression responses of preform in vacuum infusion process. *Chinese Journal of Aeronautics, 21*(4), 370-377.

Zangenberg, J., Brøndsted, P., & Koefoed, M. (2014a). Design of a fibrous composite preform for wind turbine rotor blades. *Materials & Design, 56*, 635-641.

Zangenberg, J. (2013). The effects of fibre architecture on fatigue life-time of composite materials. DTU wind energy PhD-0018 (EN). (PhD theisis), Technical University of Denmark, Denmark.

Zangenberg, J., Brøndsted, P., & Gillespie, J. W. (2014b). Fatigue damage propagation in unidirectional glass fibre reinforced composites made of a non-crimp fabric. *Journal of Composite Materials, 48*(22), 2711-2727.

BUSINESS +
ECONOMY

ART +
DESIGN +
ARCHITECTURE

SCIENCE +
TECHNOLOGY

CROSSOVER

DOCTORAL
DISSERTATIONS